Biosensors and Bioelectronics 171 (2021) 112712

Contents lists available at ScienceDirect

Biosensors and Bioelectronics

journal homepage: http://www.elsevier.com/locate/bios

Recent advances in biosensors for in vitro detection and in vivo imaging of DNA methylation

Qian Zhang [a,1], Yanxia Wu [b,1], Qinfeng Xu [c], Fei Ma [a,**], Chun-yang Zhang [a,*]

[a] College of Chemistry, Chemical Engineering and Materials Science, Collaborative Innovation Center of Functionalized Probes for Chemical Imaging in Universities of Shandong, Key Laboratory of Molecular and Nano Probes, Ministry of Education, Shandong Provincial Key Laboratory of Clean Production of Fine Chemicals, Shandong Normal University, Jinan, 250014, China

[b] Department of Pathology and Pathological Diagnosis & Research Center, Affiliated Hospital of Guangdong Medical University, Zhanjiang, 524001, China

[c] School of Food and Biological Engineering, National R&D Center for Goat Dairy Products Processing Technology, Shaanxi University of Science and Technology, Xi'an, 710021, China

ARTICLE INFO

Keywords:
DNA methylation
Epigenetics
Biosensor
In vitro detection
In vivo imaging

ABSTRACT

DNA methylation is the predominant epigenetic modification that participates in many fundamental cellular processes through posttranscriptional regulation of gene expression. Aberrant DNA methylation is closely associated with a variety of human diseases including cancers. Therefore, accurate and sensitive detection of DNA methylation may greatly facilitate the epigenetic biological researches and disease diagnosis. In recent years, a series of novel biosensors have been developed for highly sensitive detection of DNA methylation, but an overview of recent advances in biosensors for in vitro detection and especially live-cell imaging of DNA methylation is absent. In this review, we summarize the emerging biosensors for in vitro and in vivo DNA methylation assays in the past five years (2015–2020). Based on the signal types, the biosensors for in vitro DNA methylation assay are classified into five categories including fluorescent, electrochemical, colorimetric, surface enhanced Raman spectroscopy, mass spectrometry, and surface plasmon resonance biosensors, while the biosensors for in vivo DNA methylation assay mainly rely on fluorescent imaging. We review the strategies, features and applications of these biosensors, and provide a new insight into the challenges and future directions in this area.

1. Introduction

Epigenetics is defined as heritable and revisable change in gene expression without the involvement of any changes in DNA sequence, and it mainly includes DNA/RNA methylation, RNA silencing, histone modification, noncoding RNAs, and chromosome remodeling (Campuzano et al., 2019; Cavalli and Heard, 2019; Greally, 2018; Holliday, 1987; Kouzarides, 2007; Pal and Tyler, 2016). Among them, the DNA methylation occurring at cytosine in CpG island is regarded as the predominant epigenetic modification in mammals (Cheng and Roberts, 2001; Field et al., 2018; Koch et al., 2018; Neri et al., 2017), which consists of four types of methylated bases including 5-methylcytosine (5-mC), 5-hydroxymethylcytosine (5-hmC), 5-formylcytosine (5-fC), and 5-carboxycytosine (5-caC) (Kitsera et al., 2017), with the 5-mC being the most abundant DNA methylation type and accounting for approximate 1% of the total DNA bases. The abundance of 5-hmC is 10 to 100-fold lower than that of 5 mC, and the abundance of 5-fC and 5-caC is 40- to 1000-fold lower than that of 5hmC, respectively (Liu et al., 2019b; Povedano et al., 2019). The methylation of gene at the promoter region can recruit methylation binding proteins (MBPs) to prevent the binding of transcription factors and RNA polymerase to the promoter, resulting in the repression of gene transcription (Chen et al., 2017b). The normal DNA methylation participates in a variety of cellular processes such as embryonic development, genomic imprinting, cellular differentiation, and X chromosome inactivation (Bird, 2002; Reik et al., 2001). However, the abnormal DNA methylation at both locus-specific and global level induces the deregulation of gene expression (Issa, 2004) and causes a variety of human diseases such as

* Corresponding author.
** Corresponding author.
E-mail addresses: flyma100@163.com (F. Ma), cyzhang@sdnu.edu.cn (C.-y. Zhang).
[1] These authors contributed equally.

https://doi.org/10.1016/j.bios.2020.112712
Received 26 August 2020; Received in revised form 25 September 2020; Accepted 7 October 2020
Available online 8 October 2020

lung cancer, liver cancer, kidney cancer, breast cancer, and cervical cancer (Boltze et al., 2003; Das and Singal, 2004; Esteller et al., 2001; Laird, 2003; Miyamoto et al., 2005; Vanaja et al., 2009). For example, at the regional level, the methylation of *HIF3A* promoter is associated with insulin resistance and obesity (Wang et al., 2016a; Zhang et al., 2019); DNA methylation in the *NCAPH2/LMF2* promoter region is linked to Alzheimer's disease (Shinagawa et al., 2016); PGC-1α promoter methylation is association with Parkinson's disease (Su et al., 2015b). Moreover, at the global level, the global DNA methylation decreases in Alzheimer's disease patients (Chouliaras et al., 2013); the global loss of DNA methylation is linked to kidney cancer (Chen et al., 2016) and ovarian cancer (Tucker et al., 2018), and the global increase in DNA methylation levels is observed in osteoarthritic chondrocytes (Taylor et al., 2014). Consequently, the detection of methylation events at both regional and global levels is crucial to physiological and pathological researches. In addition, the alternation of DNA methylation level can be applied for the classification of central nervous system tumors (Capper et al., 2018) and the discrimination of intracranial tumors (Nassiri et al., 2020), suggesting that DNA methylation may serve as the important biomarker for disease diagnosis and treatment. Therefore, there is an urgent need to develop efficient, selective and sensitive biosensors for DNA methylation assay.

The conventional methods for DNA methylation assay mainly rely on bisulfite conversion and methylation-sensitive restriction endonuclease (MSRE) digestion (Nazmul Islam et al., 2017; Syedmoradi et al., 2016; Taleat et al., 2015; Zhang et al., 2015). The bisulfite conversion assay is currently considered to be the gold standard method for the detection of DNA methylation, and it can convert cytosine to uracil, with methylcytosine remaining unchanged (Rohde et al., 2008). It enables the detection of methylcytosine (mC) at a single base resolution and at any methylation sites. However, the process of bisulfite conversion is cumbersome and time-consuming, and may even lead to DNA degradation and incomplete conversion that can produce false positivity (Tanaka and Okamoto, 2007). The MSREs are a class of enzymes that can recognize and cleave the DNAs which contain unmethylated cytosine sites, but it will not digest the methylated DNAs (Ramsahoye et al., 1997). In comparison with the bisulfite conversion methods, the MSRE digestion-based methods have significant advantages of mild reaction conditions and simple operation. Nevertheless, only few MSREs (e.g., HpaII and GlaI) are now available, resulting in the impossibility for the detection of all DNA methylation sites. In addition, false positivity can arise due to the incomplete MSRE digestion (Dahl and Guldberg, 2003). Based on above two strategies, a variety of DNA methylation assays have been established, such as MSRE-polymerase chain reaction (PCR)/Souther (Liang et al., 2002; Singer-Sam et al., 1990), bisulfite sequencing PCR (BSP) (Frommer et al., 1992; Susan et al., 1994), methylation specific PCR (MSP) (Herman et al., 1996), methylation-sensitive single-nucleotide-primer extension (Ms-SnuPE) (Gonzalgo and Jones, 1997), and the combined bisulfite restriction analysis (COBRA) (Xiong and Laird, 1997). Among them, the MSRE-PCR/Southern is straightforward, but it involves large DNA sample consumption and is prone to false positivity due to the incomplete digestion (Fraga and Esteller, 2002; Smith and Ford, 2006). BSP has high accuracy and it can be used for high-throughput methylation analysis, but it is relatively expensive and involves tedious procedures (Susan et al., 1994). Besides its features of high sensitivity and low DNA sample consumption, MSP enables the evaluation of DNA methylation status within CpG islands in a short time without the involvement of methylation-sensitive restriction enzymes, but it may suffer from false positivity due to the incomplete bisulfite treatment (Deng et al., 1999; Li et al., 1999). The Ms-SnuPE can quantitatively detect DNA methylation levels with the involvement of only a small amount of DNA sample, but the use of radioactive isotopes limits its wide applications (Gonzalgo and Jones, 1997). The COBRA is simple, rapid and quantitative, but it can only detect the methylation status which has a specific restriction enzyme site (Goedecke et al., 2009; Karpinski et al., 2012).

In recent years, a series of novel biosensors have been developed by the integration of novel analytical methods (e.g., FÖrster resonance energy transfer, single-molecule detection, exponential amplification reaction, ligase chain reaction, hybridization chain reaction, paired-end tagging, supersandwich DNA structure assembly, reverse-Hoogsteen hydrogen bonding, synthetic-molecule/protein hybrid probe, split fluorophore) and nanomaterials (e.g., quantum dot, gold nanoparticle, upconversion nanoparticle, graphene oxide, gold nanorod) to improve the performance of DNA methylation assays and meanwhile expand their applications to the live-cell imaging. However, an overview of recent advances in DNA methylation biosensors is absent. In this review, we review the advances in biosensors for in vitro detection and in vivo imaging of DNA methylation in the last five years (2015–2020). Because 5-mC is the most abundant and most widely studied methylation type, this review mainly focuses on the biosensors for 5-mC detection. The biosensors for in vitro detection of DNA methylation are categorized into five types including fluorescent (Ma et al., 2015; Sun et al., 2018; Wang et al., 2018; Wu et al., 2016; Xu et al., 2016), electrochemical (Chen et al. 2017a, 2019; Feng et al. 2019, 2020; Huang et al., 2019; Wang et al., 2017b), colorimetric (Li et al., 2018; Su et al., 2015a), surface enhanced Raman spectroscopy (Wang et al., 2015, 2016b), mass spectrometry (Lin et al., 2016), and surface plasmon resonance (Huertas et al., 2018), while the biosensors for in vivo imaging of DNA methylation are mainly based on fluorescent imaging (Hori et al., 2018; Lungu et al., 2017). We will review the principles, features and applications of these biosensors, and discuss the challenges and future directions in this area as well.

2. In vitro DNA methylation biosensors

2.1. Fluorescent biosensors for DNA methylation assay

Fluorescence detection is the most popular analytical method in bioanalysis applications due to its high sensitivity and easy operation (Ding and Tian, 2015; Li et al., 2010a). With inorganic nanomaterials (Ma et al., 2015; Wu et al., 2016) and organic dyes (Sun et al., 2018; Xu et al., 2016) as the fluorescence indicators, a series of homogeneous (separation-free) and heterogeneous (separation-assisted) biosensors have been constructed for sensitive and selective detection of DNA methylation (Ma et al., 2015; Sun et al., 2018; Wu et al., 2016; Xu et al., 2016).

FÖrster resonance energy transfer (FRET) is a non-radiative energy transfer process from the donor fluorophore with high energy to the acceptor fluorophore with lower energy (Andrew and Barnes, 2000). The FRET strongly depends on the center-to-center separation distance, and it requires a non-zero integration of spectral overlap between the donor emission and the acceptor absorption. FRET enables the homogenous target detection without separation steps (Masters, 2008; Stryer, 1978). Quantum dots (QDs) are a new type of semiconductor nanocrystals with the merits of broad and continuous distribution of excitation spectra, narrow and symmetrical emission spectra, large Stokes shift, high molar extinction coefficient, high quantum yield, good photostability and long fluorescence lifetime (Ma et al., 2018; Resch-Genger et al., 2008; Zhou et al., 2013). Mao et al. reported a QD-based FRET biosensor for sensitive detection of DNA methylation using the QD as the FRET donor (Ma et al., 2015). As shown in Fig. 1A, in the presence of endonuclease HpaII, the methylated DNA remains unchanged. The unchanged methylated DNA is subsequently amplified by PCR to produce multiple Alexa Fluor 647 (A647)-labeled DNA products through the incorporation of A647-dNTPs. These A647-labeled PCR products can bind the QDs through electrostatic interactions, resulting in efficient FRET from the QD to A647. In contrast, the unmethylated DNA will be digested by endonuclease HpaII, and consequently no PCR reaction occurs and no A647-labeled DNA binds the QD to cause FRET. This biosensor can detect DNA methylation levels of three tumor suppressor genes including *PCDHGB6*, *HOXA9* and *RASSF1A* in lung cancer tissues.

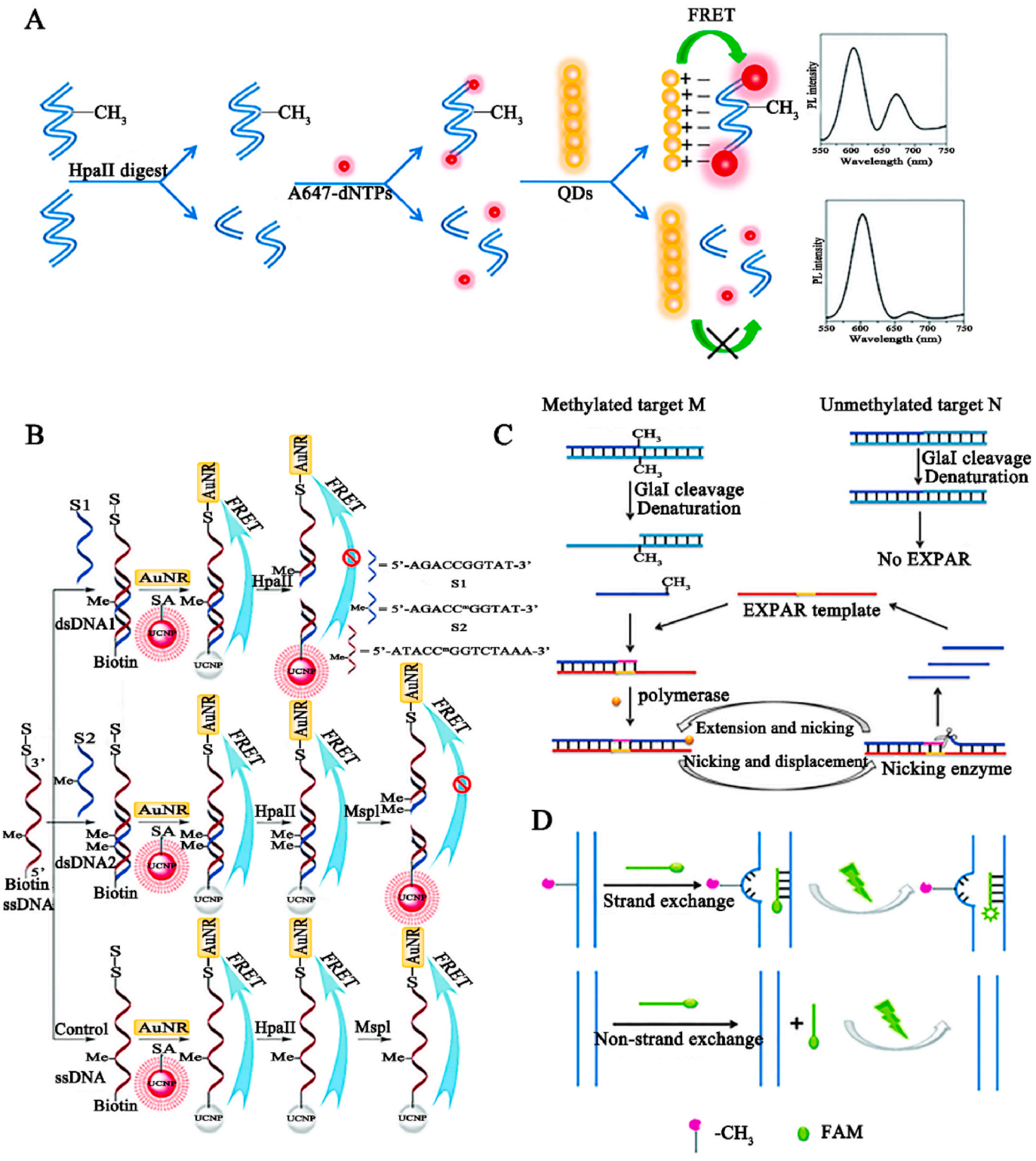

Fig. 1. (A) Schematic illustration of QD-based fluorescent biosensor for the detection of DNA methylation. Reproduced from Ma et al. (2015) with permission from The Royal Society of Chemistry. (B) Schematic illustration of UCNP and AuNR-based fluorescent biosensor for the detection of DNA methylation. Reproduced from Wu et al. (2016) with permission from The Royal Society of Chemistry. (C) Schematic illustration of EXPAR-based fluorescent biosensor for the detection of DNA methylation. Reproduced from Sun et al. (2018) with permission from The Royal Society of Chemistry. (D) Schematic illustration of enzyme-free fluorescent biosensor for the detection of DNA methylation. Reproduced from Xu et al. (2016) with permission from The Royal Society of Chemistry.

Moreover, the use of the dye-labeled nucleotide triphosphates instead of the dye-labeled DNA probes can greatly simplify the assay design and reduce the assay cost.

Lanthanide-doped fluoride upconversion nanoparticles (UCNPs) have distinct optical properties including good photochemical stability, scarce photobleaching/blinking, minimal autofluorescence background, large anti-Stokes shift and good biocompatibility (Wu et al., 2009). Moreover, UCNPs exhibit high emission in the visible region (Wang

et al., 2005), while gold nanorods (AuNRs) have strong absorption in the visible region (Storhoff et al., 1998). Therefore, UCNPs and AuNRs can serve as the FRET donors and the FRET acceptors, respectively. Guo et al. developed a fluorescent biosensor based on FRET between UCNPs and AuNRs for the detection of DNA methylation (Wu et al., 2016). As shown in Fig. 1B, a methylated ssDNA is labeled with biotin at the 5′ end and disulfide at the 3′ end, and it can hybridize with the methylated target strand S2 to form a double-stranded dsDNA2. The dsDNA can subsequently bind with the streptavidin-labeled UCNPs and AuNRs through streptavidin-biotin interaction and S–Au bond formation to obtain the UCNPs-dsDNA2-AuNRs complex. Upon the addition of endonuclease HpaII, the dsDNA2 remains unchanged, resulting in efficient FRET between the UCNPs and the AuNRs. When methylated target S1 is present, the UCNPs-dsDNA1-AuNRs is formed. Because the dsDNA1 is sensitive to endonuclease HpaII, the UCNPs-dsDNA1-AuNRs complex is destroyed by HpaII, leading to no occurrence of FRET between the UCNPs and the AuNRs. This biosensor enables the simple and sensitive detection of DNA methylation with a limit of detection as low as 7 pM, without the involvement of PCR amplification.

Nucleic acid amplification is able to efficiently amplify target signal for the improvement of assay sensitivity (Zhao et al., 2015). Among different nucleic acid amplification approaches, exponential amplification reaction (EXPAR) has distinct advantages of isothermal reaction temperature, high amplification efficiency, and rapid amplification kinetics, and it can achieve more than 10^6-fold signal amplification within a short time (Liu et al., 2018b; Ma et al., 2014). Li et al. developed a EXPAR-based fluorescent biosensor for specific and sensitive detection of DNA methylation (Sun et al., 2018). As shown in Fig. 1C, endonuclease GlaI can specifically recognize methylated DNA target M and cleaves it in the middle of sequence GmCGmC (Tarasova et al., 2008), leading to the release of X sequence under heat denaturation. The EXPAR template X′-Y-X′ contains two repeat X′ sequences complementary with X and a recognition site for nicking endonuclease (Nt.BstNBI). The released X sequence can hybridize with the EXPAR template to initiate EXPAR in the presence of Vent (exo-) DNA polymerase, generating a dsDNA duplex with a recognition site for Nt.BstNBI. Subsequently, Nt.BstNBI nicking enzyme cleaves the upper strand of the dsDNA duplex to trigger the cyclic polymerization, generating abundant X sequences. The X sequences can hybridize with new free EXPAR templates to initiate new cycles of polymerization, nicking and strand displacement amplification, leading to exponential signal amplification. The DNA products of EXPAR can be real-time detected with SYBR Green I as the fluorescent indicator. In contrast, the unmethylated DNA target N cannot be recognized and cleaved by GlaI. As a result, the DNA target remains intact and no EXPAR is initiated. Due to the high specificity of GlaI and the high signal amplification of EXPAR, this biosensor exhibits ultrahigh sensitivity with a low detection limit of 200 aM, and it can distinguish as low as 0.01% methylation levels from the mixture.

The above-mentioned biosensors require specific enzymes for target recognition and detection, which increases both the experimental complexity and assay cost. Zhou et al. developed a simple and enzyme-free fluorescent biosensor for the detection of DNA methylation based on DNA strand exchange reaction and gel separation (Xu et al., 2016). As shown in Fig. 1D, a 21-nt ssDNA labeled with FAM serves as the detection probe. In the presence of methylated DNA, the detection probe can bind to its complementary strand of target DNA, inducing base pair exchange to form a stable heteroduplex product. As a result, the target DNA is labeled with FAM, which can be analyzed by fluorescence-based native polyacrylamide gel electrophoresis. In contrast, the detection probe cannot exchange with the unmethylated DNA, and consequently no target DNA can be labeled by FAM. This biosensor is enzyme-free, and the whole assay can be completed within 2 h under physiological conditions. Moreover, this biosensor can be applied for simultaneous detection of multiple DNA methylation sites by using different fluorescent labels.

Single-molecule fluorescence detection enables the investigation of biomolecules at the single-molecule level, and provides a simple and ultrasensitive platform for quantifying target molecules by counting the individual fluorescence signals (Song et al., 2016; Walt, 2012). In comparison with the ensemble fluorescence measurements, single-molecule fluorescence detection has advantages of high signal-to-noise ratio, high sensitivity, and low sample consumption (Hsin and Yeung, 2007; Hu and Zhang, 2014; Ma et al. 2016a, 2016b; Medintz et al., 2005; Somers et al., 2007; Wang et al., 2017a; Xu and Yeung, 1997). Zhang et al. developed a single QD-based biosensor for DNA methylation detection (Wang et al., 2018). As illustrated in Fig. 2A, two sets of DNA probes (X and Y, X′ and Y′) are employed for DNA methylation assay, with probes X and Y being complementary to target DNA sequence and probes X′ and Y′ being complementary to the sequences of probes X and Y, respectively. The methylated DNA remains unchanged after bisulfite treatment, and it can hybridize with probes X and Y to generate the ligated XY products by thermostable DNA ligase. The XY strand can serve as the template for ligating probes X′ and Y′ to generate the X'Y', and X'Y' strand may in turn act as the template for ligating probes X and Y to generate the XY. As a result of cyclic ligase chain reaction, a large number of XY products are produced. Because the phosphorothioate modification at the 3′ end of probe Y, the XY product is preserved after exonucleases I and III digestion, and it can hybridize with the capture and reporter probes to obtain the sandwich hybrids. Subsequently, the sandwich hybrids assemble on the surface of 605QDs to form the 605QD-DNA-Cy5 nanostructures through biotin-streptavidin interaction, resulting in efficient FRET between 605QD and Cy5 and consequently the emission of Cy5. The Cy5 signals can be simply quantified by total internal reflection fluorescence (TIRF)-based single molecule imaging. In contrast, when the methylated DNA is present, the cytosine is converted to uracil which cannot trigger the ligase chain reaction (Fig. 2B). As a result, neither XY strand nor the 605QD-DNA-Cy5 nanostructure is produced, and no FRET between 605QD and Cy5 occurs. This biosensor can detect DNA methylation at both CpG and non-CpG sites with single 5-mC resolution. Moreover, this biosensor exhibits high sensitivity with a detection limit of as low as 1.0 aM, and it can detect as low as 0.01% methylation level in human lung cancer cells.

2.2. Electrochemical biosensors for DNA methylation assay

Electrochemical biosensors have distinct advantages of intrinsic simplicity, low cost, field portability, and fast response time, and they enable sensitive quantification of target molecules through the measurement of coulometric, amperometric, and potentiometric signals (Feng et al., 2020; Kato et al., 2008; Krejcova et al., 2017; Li et al., 2014). A variety of electrochemical biosensors have been developed for DNA methylation assay with tetramethylbenzidine (TMB) (Chen et al. 2017a, 2019), methylene blue (MB) (Feng et al. 2019, 2020), ferrocene (Fc) (Feng et al., 2019), and hydroquinone (Huang et al., 2019; Povedano et al. 2019, 2020) as the electrochemical tags.

Zhao et al. developed a paired-end tagging-based electrochemical biosensor for the detection of DNA methylation (Chen et al., 2017a). As shown in Fig. 3A, upon the treatment of $NaHSO_3$, the methylated DNA remains unchanged and it can be amplified by PCR using 5′-digoxigenin (Dig)-labeled forward primer and 5′-biotin-labeled reverse primer. The resultant DNA products with paired-end tagging (i.e., Dig and biotin) are captured by anti-Dig-modified Au electrode and subsequently bind with avidin-labeled-horseradish peroxidase (HRP) to form the Au-DNA-HRP structure. HRP is able to catalyze the oxidization of tetramethylbenzidine (TMB) to generate a distinct electrochemical signal. In contrast, the $NaHSO_3$ treatment of unmethylated DNA enables the conversion of cytosine to uracil, and the resultant DNA cannot be recognized by primer for the initiation of PCR amplification. As a result, no Au-DNA-HRP structure is formed and no electrochemical signal is generated. This biosensor is simple and sensitive, and it can identify as little as 40 pg of methylated genomic DNA and distinguish as low as 1% methylation

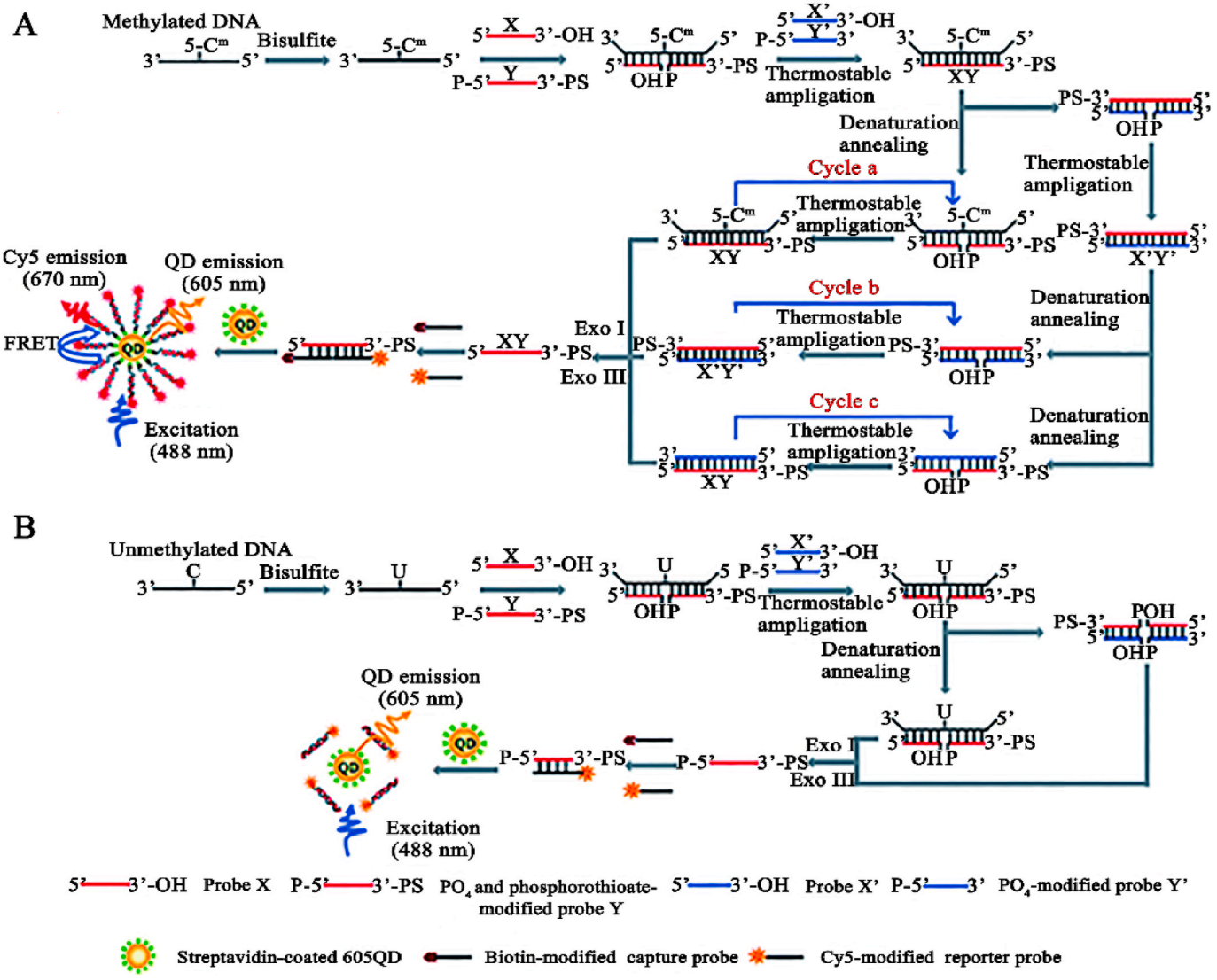

Fig. 2. Scheme illustration of a single-QD-based fluorescent biosensor for the detection of DNA methylation. Reproduced from Wang et al. (2018) with permission from The Royal Society of Chemistry.

level from the mixture. Moreover, this biosensor can detect tumor-specific DNA methylation in clinical serum samples with 91% sensitivity.

It should be noted that PCR reaction requires a sophisticated thermocycler to precisely control the reaction temperature. Alternatively, the exonuclease III (Exo III) digest reaction can be carried out under isothermal conditions, and it can be used to construct target recycling-based signal amplification strategy with high sensitivity, simple assay design, and ease operation protocol (Liu et al. 2018c, 2019a, 2020). Wang et al. developed an Exo III-assisted target recycling-based electrochemical biosensor to detect DNA methylation (Feng et al., 2020). As shown in Fig. 3B, the DNA probe with stem-loop structure is modified with MB tag at the 5′ end and immobilized on the surface of nano-Au-modified glassy carbon electrode (GCE) through Au–S bond. The auxiliary DNA can partially hybridize with the DNA probe to break its stem-loop structure, resulting in the separation of MB from the GCE surface and consequently the decrease of electrochemical signal. Upon $NaHSO_3$ treatment, the methylated DNA remains unchanged, and it can bind with auxiliary DNA to initiate the Exo III-assisted cycling digestion of auxiliary DNAs, facilitating the restoring of the stem-loop structure of probe DNA which brings MB tag into close proximity with the GCE surface for the generation of a distinct electrochemical signal. In contrast, when the unmethylated DNA is treated with $NaHSO_3$, cytosine is converted to uracil which hybridizes with auxiliary DNA to form a mismatched dsDNA. Because Exo III exhibits significantly reduced cleavage activity toward the mismatched dsDNA (Liu et al., 2018c), few auxiliary DNA can be digested, leading to a weak electrochemical signal. Due to the efficient Exo III-assisted signal amplification, this biosensor enables the sensitive detection of DNA methylation with a detection limit of 4 fM, and it can be further applied for accurate detection of DNA methylation in human serum samples.

To improve the detection specificity, Zhao et al. developed a tetrahedral DNA-based electrochemical biosensor to detect methylated DNA (Wang et al., 2017b). The use of tetrahedral DNA as the capture probes can significantly increase target accessibility and minimize the non-specific adsorption due to the rigid scaffold, ordered orientation and well controlled spacing (Ge et al., 2014; Liang et al., 2014; Liu et al., 2018a). As shown in Fig. 3C, the circulating DNA is extracted and converted with $NaHSO_3$ treatment, and the unchanged methylated DNA can be discriminated using biotin-labeled primers and subsequently amplified through asymmetric methylation-specific PCR (AMSP), producing a large number of biotin-labeled ssDNA products. The tetrahedral DNA probes can be self-assembled on a gold electrode surface via Au–S bond, and they can capture the biotin-labeled ssDNA products through

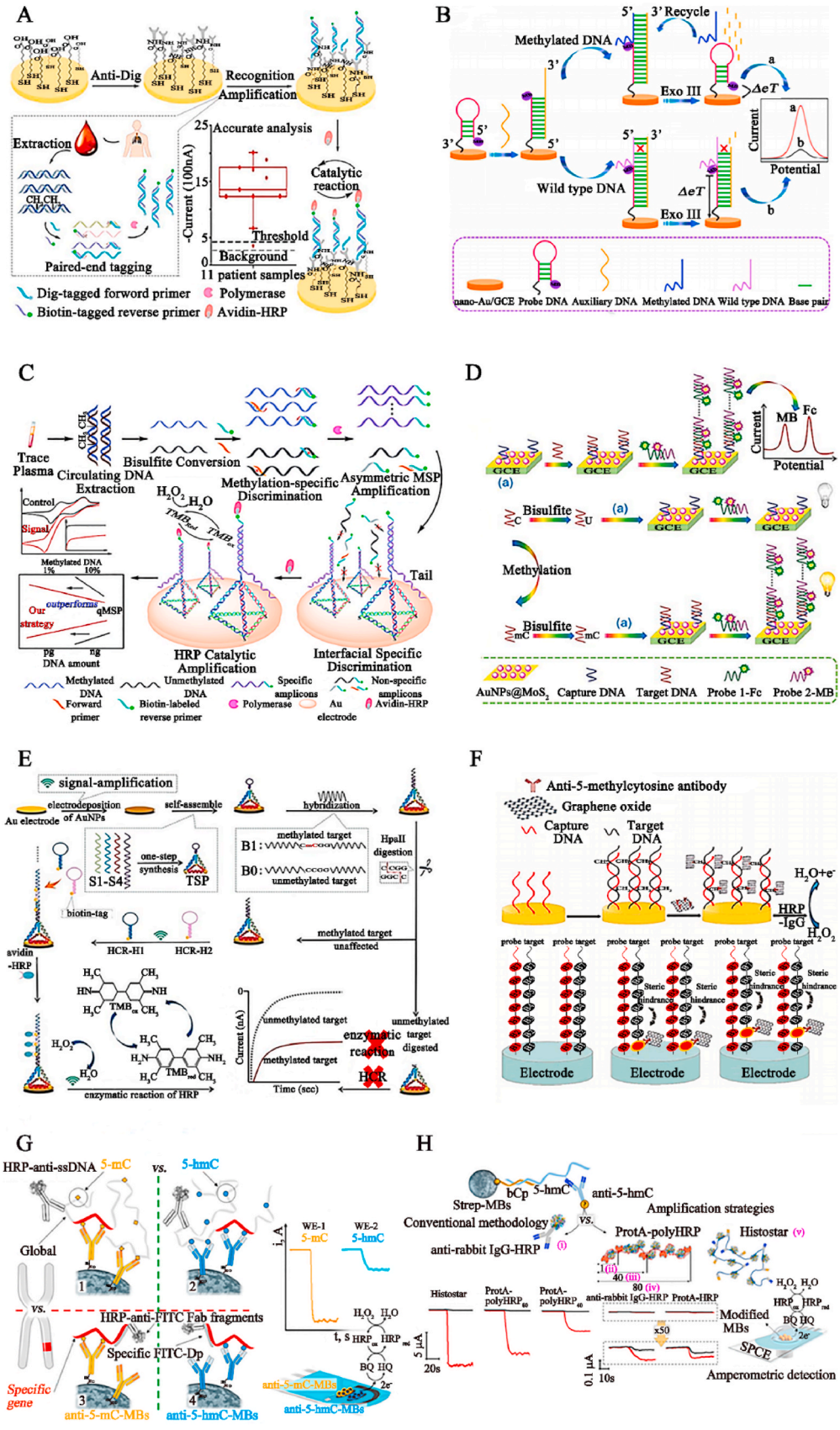

Fig. 3. (A) Schematic illustration of paired-end tagging-based electrochemical biosensor for DNA methylation assay. Reproduced from Chen et al. (2017a) with permission from American Chemical Society. (B) Schematic illustration of Exo III-assisted target recycling-based electrochemical biosensor for DNA methylation assay. Reproduced from Feng et al. (2020) with permission from Elsevier B.V.. (C) Schematic illustration of tetrahedral DNA-based electrochemical biosensor for DNA methylation assay. Reproduced from Wang et al. (2017b) with permission from The Royal Society of Chemistry. (D) Schematic illustration of supersandwich DNA structure assembly-based electrochemical biosensor for DNA methylation assay. Reproduced from Feng et al. (2019) with permission from American Chemical Society. (E) Schematic illustration of electrochemical biosensor based on hybridization chain reaction and tetrahedral DNA for DNA methylation assay. Reproduced from Chen et al. (2019) with permission from American Chemical Society. (F) Schematic illustration of GO-based electrochemical biosensor for DNA methylation assay. Reproduced from Huang et al. (2019) with permission from Elsevier B.V.. (G) Magnetic beads-based electrochemical biosensor for simultaneous detection of 5 mC and 5-hmC methylation. Reproduced from Povedano et al. (2019) with permission from American Chemical Society. (H) Magnetic beads-based electrochemical biosensor for the detection of 5-hmC methylation. Reproduced from Povedano et al. (2020) with permission from American Chemical Society.

specific base pairing. Subsequently, the avidin-conjugated HRP can bind with the ssDNA products through avidin-biotin interaction, and they can oxidize TMB to generate a distinct electrochemical signal. In contrast, the cytosine of unmethylated DNA is converted to uracil upon $NaHSO_3$ treatment, which is not complementary to the primers, leading to no occurrence of AMSP. As a result, no biotin-labeled ssDNA product is produced and no electrochemical signal is detected. In this biosensor, the AMSP significantly reduces the primer dimer artifacts and the tetrahedral DNA probes dramatically inhibit the non-specific adsorption of amplification byproducts, enabling the identification of single-copy methylated DNA even in the presence of more than 1000-fold unmethylated alleles.

It should be noted that polymerase and Exo III involved in above electrochemical biosensors are relatively expensive and require strict experimental conditions. Wang et al. developed a supersandwich DNA structure assembly-based electrochemical biosensor for sensitive detection of DNA methylation without PCR amplification (Feng et al., 2019). The supersandwich DNA structure assembly is a kind of hybridization chain reaction that can achieve enzyme-free signal amplification through target-induced cascaded self-assembly of two liner DNA probes (Jiang et al., 2012; Liu et al., 2013). As shown in Fig. 3D, the electrode surface is coated with Au nanoparticle-modified MoS_2 nanocomposites (AuNPs@MoS2) to improve both the charge-transfer efficiency and the capture DNA loading ratio. Upon $NaHSO_3$ treatment, the methylated DNA remains unaltered, and it can hybridize with the capture DNA probe to form a partially complementary dsDNA which enables the capture of ferrocene-labeled probe 1 (probe 1-Fc) and methylene blue-labeled probe 2 (probe 2-MB) through cascaded hybridization chain reaction. As a result, multiple Fc and MB molecules are brought close to the electrode surface, generating a distinct current signal in a dual-signal manner. In contrast, the cytosine of unmethylated DNA is converted to uracil which cannot bind with capture DNA probe to initiate the hybridization chain reaction. Consequently, neither Fc nor MB is captured, and no electrochemical signal is detected. This biosensor possesses high accuracy due to dual-signal readout of two independent potentials (Fc and MB) and efficient signal amplification originated from supersandwich DNA structure assembly, and it can achieve a low detection limit of 450 aM without the involvement of any enzymatic reaction. Moreover, this biosensor can accurately quantify methylated DNA extracted from human blood serum samples.

Taking advantages of tetrahedral DNA probe and hybridization chain reaction, Zheng et al. developed an electrochemical biosensor for ultrasensitive detection of DNA methylation (Chen et al., 2019). As shown in Fig. 3E, the tetrahedral DNA nanostructure probe (TSP) with a capture probe sequence at the vertice is immobilized on the Au nanoparticle (AuNP)-coated electrode. The methylated DNA B1 remains intact after treatment with restriction endonuclease HpaIII, and it can hybridize with the capture probe of TSP to trigger hybridization chain reaction (HCR) between two biotin-tagged probes (i.e., HCR-H1 and HCR-H2). As a result, multiple biotin moieties are brought close to the electrode surface and subsequently bind with HRP, which in turn oxidize TMB to generate a distinct electrochemical signal. In contrast, the unmethylated DNA B0 will be completely digested by restriction endonuclease HpaII, resulting in neither the occurrence of HCR reaction nor the generation of an electrochemical signal. This biosensor exhibits good specificity, excellent stability, and high sensitivity with a detection limit of 0.93 aM, and it possesses a wide dynamic range of 6 orders of magnitude from 1 aM to 1 pM.

The graphene oxide (GO) obtained by the oxidation of graphite is a novel carbon material with large surface area and considerable functional groups (e.g. hydroxyl and carboxyl), and it can be easily conjugated with various functional probes for the development of different biosensors (Feng et al., 2020; Kudr et al., 2020; Zhou et al., 2009). Zheng et al. developed a GO-based electrochemical biosensor for DNA methylation assay (Huang et al., 2019). As shown in Fig. 3F, the capture DNA is immobilized on the electrode surface via Au–S bond. When methylated DNA hybridize with capture DNA, the anti-5-methylcytosine (5 mC) antibody-modified GO will specifically bind with CpG methylation sites through immune recognition. The immunoglobulin G (IgG) labeled with HRP can subsequently bind with anti-5mC antibody, facilitating the capture of HRP by the electrode. The captured HRP can catalyze the oxidation of hydroquinone to benzoquinone, generating a distinct electrochemical signal. In contrast, the unmethylated DNA does not have CpG methylation site, and neither anti-5mC antibody-modified GO nor HRP-labeled HRP can be captured for the generation of an electrochemical signal. This biosensor employs anti-5mC antibody for methylation site discrimination, eliminating the use of complicated bisulfite treatment and enzyme digestion. Moreover, this biosensor is very sensitive with a detection limit of 1 fM.

The Campuzano and Pingarrón's group developed a magnetic beads (MBs)-based PCR-free and bisulfite treatment-free electrochemical biosensor for DNA methylation assay (Povedano et al., 2019). As shown in Fig. 3G, the methylated ssDNA can be captured by DNA methylation-specific antibody-modified MBs and labeled with HRP-anti-ssDNA antibody and FITC-Dp/HRP-anti-FITC Fab fragments. The resultant bioconjugates are then magnetically assembled on the surface of screen-printed carbon electrodes (SPCEs) to generate a distinct electrochemical signal via the HRP-catalyzed oxidation of hydroquinone by H_2O_2. This biosensor can simultaneously detect 5 mC and 5-hmC at both global and gene-specific levels, and the whole assay can be completed in less 90 min with good reproducibility. Moreover, this biosensor can be successfully applied for the detection of DNA methylation in colorectal tissues and cells and even serums from breast and lung cancer patients.

Recently, Campuzano and Pingarrón's group developed a MBs-based electrochemical biosensor for the detection of 5-hmC methylation at localized sites (Povedano et al., 2020). As shown in Fig. 3H, the biotinylated complementary probe (bCp) is conjugated to streptavidin−MB via biotin-streptavidin interaction, and the anti-5-hmC antibody is modified with multiple HRPs by using commercial bioreagents ProtA−polyHRP$_{80}$ and Histostar. The target 5-hmC methylation target can be captured by MB through the hybridization with bCp and subsequently binds to HRPs-modified anti-5-hmC antibody through immune recognition. The resultant MB-HRPs bioconjugates are then magnetically assembled on the surface of SPCEs to generate an electrochemical signal via HRP-catalyzed oxidation of hydroquinone by H_2O_2. Notably, the use of ProtA−polyHRP$_{80}$ and Histostar for the labeling of single antibody with multiple HRPs can achieve an amplification factor of 43.6 and 55.2, respectively, enabling the detection of 5-hmC with single-base sensitivity. This biosensor can be applied for the detection of 5-hmC methylation in *MGMT* promoter extracted from cells and tissues of colorectal cancer patients.

2.3. Colorimetric biosensors for DNA methylation assay

The colorimetric biosensor enables target detection through direct observation of the color change by the naked eye, and it has significant advantages of easy operation, fast response, low cost, and simple instrumentation (Elghanian et al., 1997). The aggregation of gold nanoparticles (AuNPs) (Su et al., 2015a) and the formation of HRP-mimicking DNAzymes (Li et al., 2018) have been used as the efficient strategies to develop the colorimetric biosensors for DNA methylation assay.

Apart from functioning as the DNA probe carrier in the supersandwich DNA structure assembly-based electrochemical biosensor, the AuNPs possess high extinction coefficient and unique size- and distance-dependent color changes, making them promising in the construction of colorimetric biosensors (Elghanian et al., 1997; Rosi and Mirkin, 2005). Li et al. developed a AuNP-based colorimetric biosensor for DNA methylation assay (Su et al., 2015a). In this biosensor, ligase chain reaction (LCR) is introduced to improve the detection sensitivity. LCR facilitates the exponential signal amplification via thermostable DNA

ligase-assisted cyclical DNA ligation reaction to achieve comparable sensitivity as PCR (Barany, 1991; Ma et al., 2019). As shown in Fig. 4A, after treatment of methylated DNA target M with sodium bisulfite ($NaHSO_3$), the methylcytosine remains unchanged. Consequently, probes A and probe B can hybridize with target M at the position of methylcytosine, followed by ligation by DNA ligase to form the AB strand. The obtained AB strand can serve as new template to ligate probe A′ and probe B′ to produce A'B' strand. Through cyclic ligation, denaturation and hybridization, the LCR amplification is achieved for the generation of abundant AB/A'B' dsDNA products. Because the 3′ end of probe B′ is modified with phosphorothioate, the A'B' strand is preserved after Exonuclease I and Exonuclease III digestion. The remained A'B' strand can hybridize with the AuNP-labeled A strand and the AuNP-labeled B strand, inducing the aggregation of AuNPs accompanied

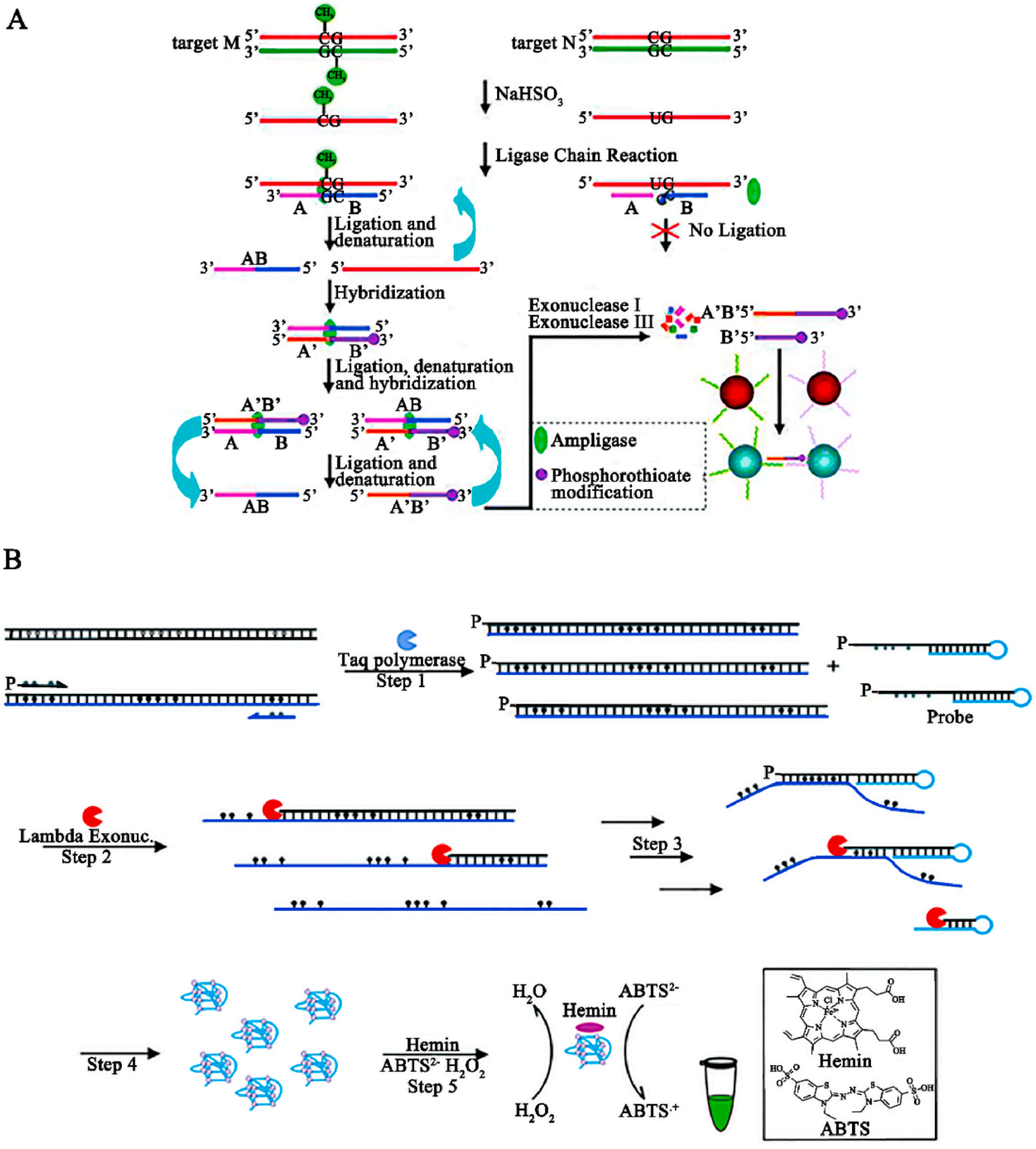

Fig. 4. (A) Schematic illustration of the AuNP-based colorimetric biosensor for DNA methylation assay. Reproduced from Su et al. (2015a) with permission from The Royal Society of Chemistry. (B) Schematic illustration of the DNAzyme-based colorimetric biosensor for DNA methylation assay. Reproduced from Li et al. (2018) with permission from The Royal Society of Chemistry.

by the color change from red to blue. In contrast, when the unmethylated DNA target N is treated with $NaHSO_3$, the cytosine is converted to uracil which is not complementary to probe A, resulting in no occurrence of LCR reaction. Consequently, the AuNPs remain dispersed and no color change is observed. This biosensor enables visual detection of DNA methylation with a low detection limit of 0.01 fM, and it can even detect 0.1% methylated DNA in the presence of large amounts of unmethylated DNAs. Moreover, this biosensor does not require any expensive instruments, facilitating its applications in common laboratories.

The G-quadruplex DNAzymes are catalytic ssDNA molecules with enhanced horseradish peroxidase (HRP)-mimicking activity, and they can catalyze the oxidation of 2,2′-azino-bis(3-ethylbenzthiazoline-6-sulfonic acid) diammonium salt (ABTS) to generate a distinct colorimetric signal (Li et al., 2010b). Tang et al. developed a DNAzyme-based colorimetric biosensor for DNA methylation assay (Li et al., 2018). As shown in Fig. 4B, the sodium bisulfite treatment enables the conversion of cytosine in methylated DNA to uracil, while methylcytosine remains unchanged. The 5′-phosphorylated methylation specific primers can hybridize with the methylated DNA, triggering PCR reaction to generate abundant amplification products. Because lambda exonuclease can selectively digest the 5′-phosphorylated DNA (Avci-Adali et al., 2009), the 5′-phosphorylated strand of the PCR products is digested by lambda exonuclease, releasing single-stranded DNAs without 5′-phosphorylation. The free single-stranded DNAs can subsequently bind with hairpin probes containing a blocked DNAzyme sequence to induce the digestion of blocking sequence by lambda exonuclease, generating free DNAzymes. The DNAzyme sequence can form the G-quadruplex structure to bind hemin, which exhibits peroxidase-like activity and enables the oxidization of ABTS to radical $ABTS^+$ with green color. In contrast, the methylation-specific primers are not complementary to the unmethylated DNA, leading to no occurrence of PCR reaction. As a result, DNAzyme is still blocked in hairpin probe and no color change is observed. This biosensor can be used for qualitative and semi-quantitative analysis of DNA methylation, and it can distinguish as low as $1/10^6$ of methylated DNA from the mixture. Moreover, this biosensor can be applied to detect DNA methylation in human hepatoma cell line (HepG2 cells), holding potential in clinical diagnosis.

2.4. Biosensors based on surface enhanced Raman scattering

Surface enhanced Raman spectroscopy (SERS) refers to the phenomenon that the sample is adsorbed on the surface of nanomaterial to enhance the Raman signal of sample (Kneipp et al., 1997; Schlücker, 2009; Wang and Schlücker, 2013), and it has the features of narrow spectral band, no light fading/self-quenching of fluorescent groups, and

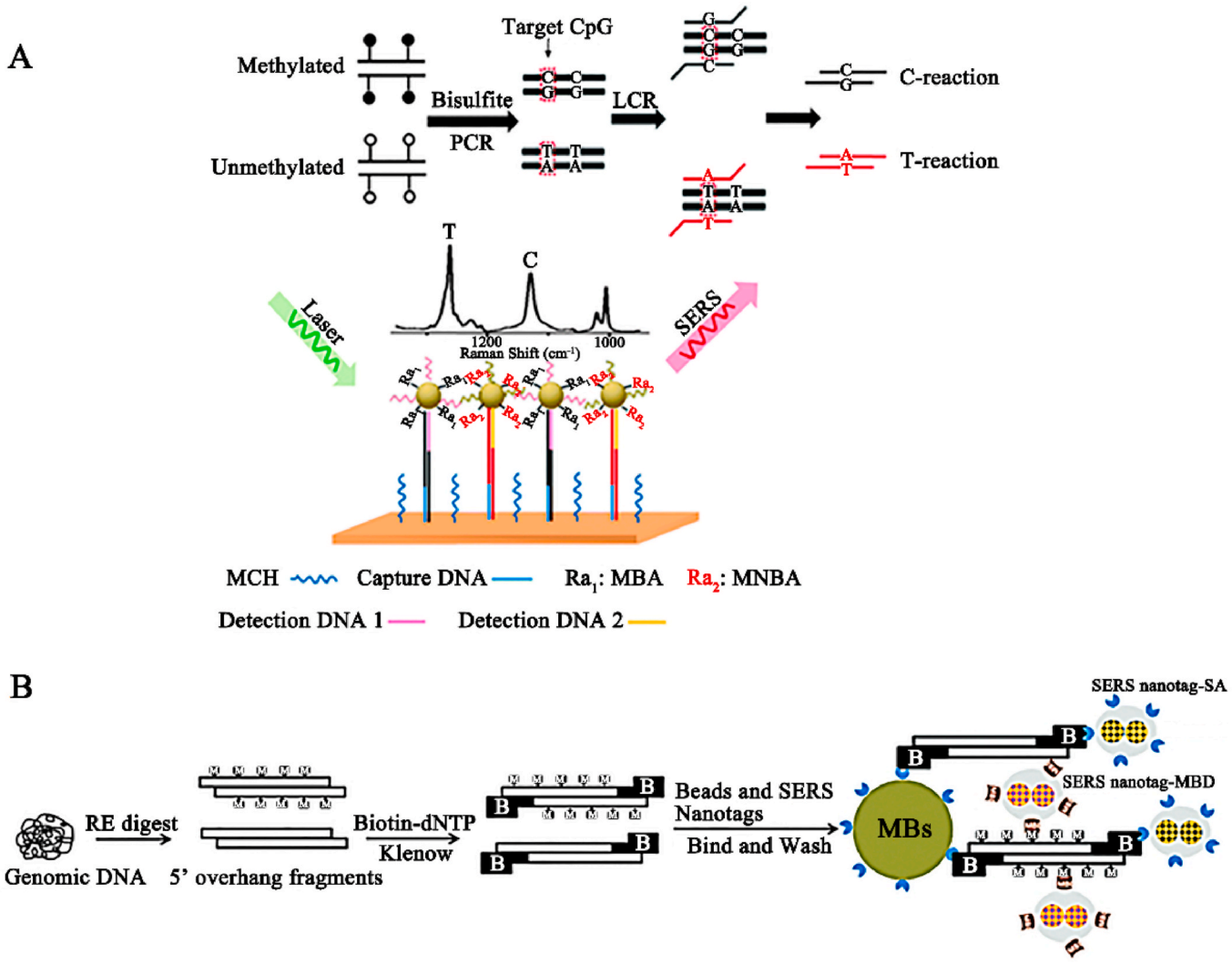

Fig. 5. (A) Schematic illustration of LCR-based SERS biosensor for multiplexed detection of DNA methylation. Reproduced from Wang et al. (2015) with permission from The Royal Society of Chemistry. (B) Schematic illustration of MBD-based SERS biosensor for the detection of DNA methylation. Reproduced from Wang et al. (2016b) with permission from The Royal Society of Chemistry.

fast analysis speed (Kneipp et al. 1997, 1999). Especially, SERS has a unique advantage over fluorescence in multiplexed detection due to the narrow and distinct bandwidths of vibrational Raman bands (Schlücker, 2009; Wang and Schlücker, 2013), while the overlap of fluorescence emission spectra greatly limits the assay multiplexing. The SERS biosensors employ AuNPs as the SERS substrates to enhance the signal of Raman reporters for sensitive detection of DNA methylation (Wang et al., 2015, 2016b).

Trau et al. integrated AuNPs with LCR to develop a SERS biosensor for multiplexed detection of DNA methylation (Wang et al., 2015). As shown in Fig. 5A, after bisulfite conversion, the methylated cytosine (C) remains unchanged, while unmethylated cytosine is converted to uracil (U). Subsequently, both methylated and unmethylated targets are amplified by PCR, followed by being further amplified using LCR. The LCR products of methylated and unmethylated targets can assemble on gold nanoparticles (AuNPs) with two Raman reporters (i.e., 4-mercapto-3-nitro benzoic acid (MNBA) and 4-mercaptobenzoic acid (MBA)) modification to generate distinguishable SERS signals, with MBA signal indicating the unmethylated DNA targets and MNBA signal indicating the methylated DNA target, respectively. This biosensor enables multiplexed detection of single-base change with a detection limit of 0.5 pM, and it can be further applied for sensitive detection of methylation in breast cancer cell lines (e.g., MDA-MB 231 cells, MDA-MB 468 cells, and HCC 1937 cells) and serum samples.

To avoid the complicated PCR and LCR amplification steps involved in the above biosensor, Trau et al. developed a amplification-free SERS biosensor for DNA methylation assay using methyl binding domain protein (MBD) (Wang et al., 2016b). The MBD has high affinity to methylated DNA in vitro and in vivo (Fatemi and Wade, 2006), and it can efficiently and directly recognize DNA methylation without the involvement of bisulfite treatment. As shown in Fig. 5B, the dimer and trimer gold nanoparticles (AuNPs) coated with silica are used as the

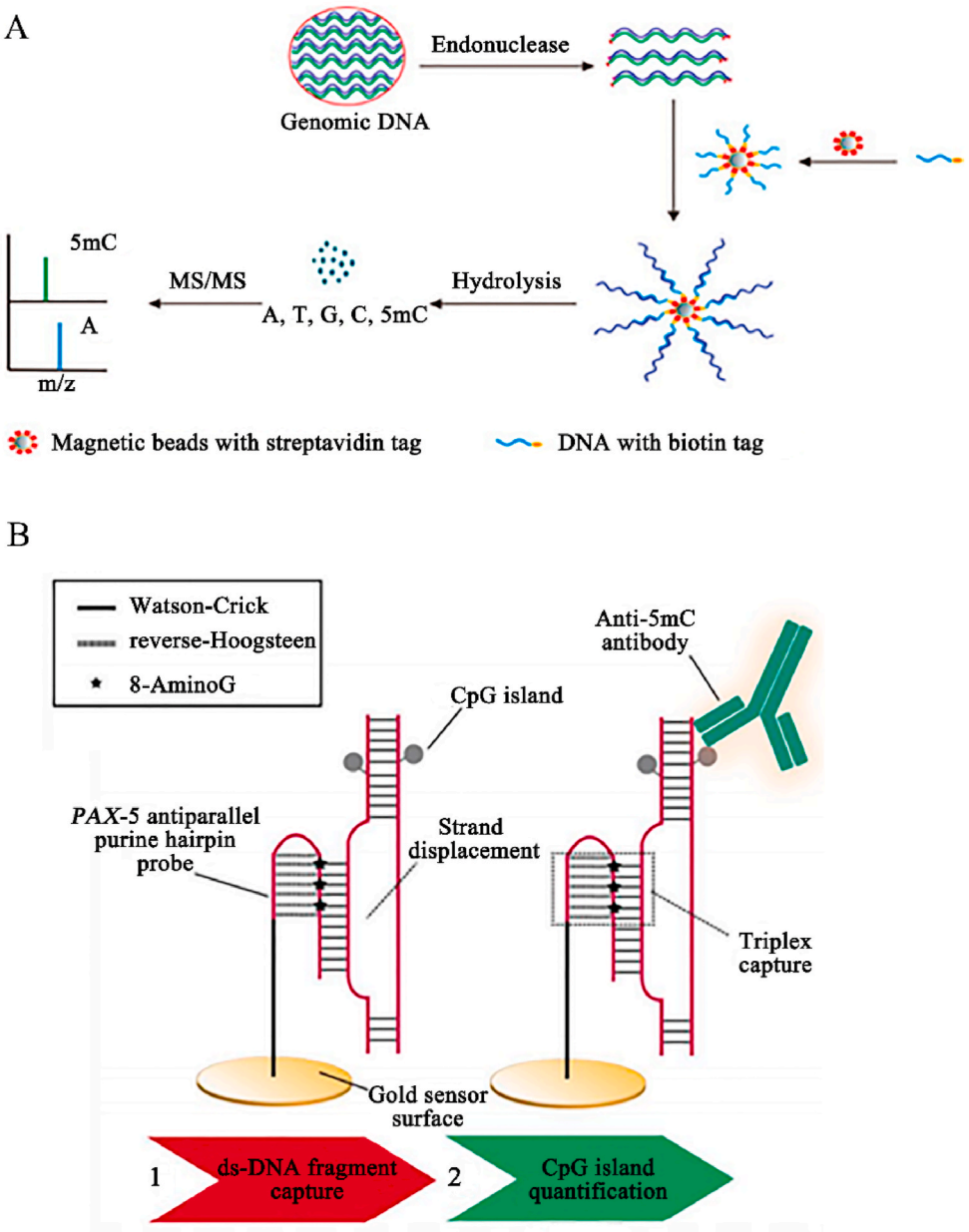

Fig. 6. (A) Schematic illustration of TFA-based MS biosensor for DNA methylation assay. Reproduced from Lin et al. (2016) with permission from American Chemical Society. (B) Schematic illustration of SPR-based biosensor for DNA methylation assay. Reproduced from Huertas et al. (2018) with permission from Elsevier B.V..

SERS substrates, and they are labeled with MBD for methyl-CpG site recognition. The genomic DNA is digested into 5′ overhang fragments by HpaII. Subsequently, biotin-dNTPs are incorporated into the DNA fragments with the assistance of Klenow DNA polymerase, generating biotin-labeled DNA fragments which can be captured by the streptavidin-magnetic beads (MB) via streptavidin-biotin interaction. The MBD-labeled SERS substrate can bind with methylated DNA fragments rather than unmethylated ones, generating distinct SERS signals after washing off the unbound SERS substrates. This biosensor can detect methylation from 0.2 ng of genomic DNA, and it can distinguish as low as 6.25% methylation level from 500 pg of total DNA. Moreover, this biosensor can be applied to detect DNA methylation in de-methylating drug-treated human cancer cell line (Jurkat cells) and breast cancer biopsy samples.

2.5. Biosensors based on mass spectrometry (MS) and surface plasmon resonance (SPR)

Mass spectrometry (MS) can provide accurate molecular weight and structure information, and possesses distinct advantages of high sensitivity, high accuracy, and high throughput (Alley et al., 2013; Angel et al., 2012; Wei et al., 2013). In recent years, MS has drawn increasing attentions in characterization of DNA/RNA damages (Wang et al., 2011) and epigenetic modifications (Fu et al., 2015). Jiang et al. developed a MS-based biosensor (named target fragmentation assay (TFA)) for ultrasensitive analysis of DNA methylation in specific sequences (Lin et al., 2016). As shown in Fig. 6A, the restriction endonucleases BbvI. is used to digest genomic DNA into small DNA fragments. The biotinylated capture probes are assembled onto the streptavidin-coated magnetic beads via streptavidin−biotin interaction to enrich the DNA fragments through magnetic separation. The resultant DNA fragments are then completely degraded into nucleobases by formic acid, and the released nucleobases containing methylated cytosine can be directly profiled by MS/MS. This biosensor exhibits high sensitivity with a detection limit of as low as 0.056 amol, and it can directly detect DNA methylation from human genomic DNA without the involvement any amplification steps. Moreover, this biosensor can be used to evaluate DNA methylation level in prostate tissue samples.

Surface plasmon resonance (SPR) enables label-free detection of target molecules in real-time with high sensitivity through measuring the change of refractive index (Aoki et al., 2019; Rich and Myszka, 2000; Zhou et al., 2019). Lechuga et al. developed a SPR-based biosensor for label-free detection of DNA methylation (Huertas et al., 2018). As shown in Fig. 6B, the detection probe is a single-stranded poly-purine reverse-Hoogsteen (PPRH) DNA containing two antiparallel poly-purine domains separated by a tetra-thymidine loop. The detection probe is immobilized on the gold surface via Au–S bond, and it can hybridize with target methylated DNA to form a triple helix through both Watson-Crick interaction and reverse-Hoogsteen hydrogen bonding. Then the anti-5mC antibody is captured by the biosensor through binding with 5 mC of methylated DNA, generating a distinct SPR signal. In contrast, unmethylated DNA does not have 5 mC, and the anti-5mC antibody cannot be captured by the biosensor for the generation of a SPR signal. This biosensor enables direct and label-free detection of DNA methylation in dsDNA with a detection limit of 115 pM, and it can be reused for up to 35 hybridization/regeneration cycles.

(Note: this part should be put after the Table 1)[a] ND: not determined. Abbreviations: AuNP, gold nanoparticle; AuNR, gold nanorod; EXPAR, exponential amplification reaction; Exo III, exonuclease III; HCR, hybridization chain reaction; LCR, ligase chain reaction; MB, magnetic bead; MBD, methyl binding domain protein; MS, mass spectrometry; POCT: point-of-care testing; PPRH, poly-purine reverse-Hoogsteen; QD, quantum dot; SERS, surface enhanced Raman spectroscopy; UCNP, upconversion nanoparticle.

2.6. Biosensors for in vivo imaging of DNA methylation

In addition to the biosensors for in vitro DNA methylation assay, several biosensors for in vivo detection of DNA methylation in living cells have been developed based on the engineered DNA methyl binding domain (MBD) (Hori et al., 2018; Lungu et al., 2017). These biosensors enables in vivo quantification of endogenous DNA methylation level and real-time monitoring of DNA methylation dynamic changes, facilitating the study of the potential roles of DNA methylation in psychological processes, disease developments, and drug responses.

Recently, Kikuchi et al. developed a fluorescent biosensor based on synthetic-molecule/protein hybrid probe for live-cell imaging of DNA methylation (Hori et al., 2018). As shown in Fig. 7A, a PYP3R-tag is fused to MBD for the construction of a synthetic-molecule/protein hybrid probe. The oxazole yellow (YO) can generate significantly enhanced fluorescence signal upon binding with DNA, and it is employed as the fluorogen (Furstenberg et al., 2007). The YO is conjugated with PYP-ligand (YOCNB) to facilitate its binding with PYP3R-tag-MBD hybrid probe. When the YO-PYP3R-tag-MBD binds with methylated DNA, the YO is brought close to DNA, generating a distinct fluorescence signal. In contrast, the YO-PYP3R-tag-MBD cannot bind with unmethylated DNA, and no enhanced signal is observed. This biosensor can be used for the imaging of DNA methylation in living NIH3T3 cells, monitoring of dynamic changes of methylated DNA during the mitosis process in real-time (Fig. 7B). Moreover, this biosensor can be applied for the screening of DNA methylation inhibitors, holding great potential in drug discovery.

Jeltsch et al. employed a split fluorophore-based bimolecular anchor detector (BiAD) to develop a fluorescent biosensor for live-cell imaging of DNA methylation (Lungu et al., 2017). As shown in Fig. 7C, this biosensor consists of an anchor module (zinc finger protein, transcription activator–like effectors, or CRISPR/dCas9) for DNA sequence-specific recognition and a detector module (MBD) for the recognition of target DNA methylation. The mVenus fluorophore is split into two non-fluorescent parts (i.e., VenN and VenC), with VenN being fused to anchor module and VenC being fused to detector module. In the absence of target DNA methylation, VenN and VenC are separated from each other, and no fluorescence signal is detected. In contrast, when target DNA is methylated, the anchor module and the detector module are close to each other, resulting in the reconstitution of a functional mVenus fluorophore and consequently the generation of a distinct fluorescence signal. This biosensor exhibits good specificity, and it enables real-time imaging of locus-specific DNA methylation changes in single NIH3T3 cell.

Besides their involvement in cell development, disease onset, and drug response, DNA methylation plays curial roles in other biological events. For example, the cadmium-induced toxicity in the red seaweed Gracilaria dura can be alleviated through the regulation of DNA methylation by selenium and spermine (Kumar et al., 2012); maternal nutrition status during early pregnancy leads to persistent and systemic DNA methylation changes of human metastable epialleles (Dominguez-Salas et al., 2014); Hop stunt viroid infection induces dynamic DNA methylation changes of ribosomal RNA genes in host cucumber (Martinez et al., 2013); the transposable element genes are demethylated upon infection of bacterial pathogen *Pseudomonas syringae* in host *Arabidopsis* (Yu et al., 2013). Therefore, the in vivo biosensors that enables real-time monitoring and tracking of DNA methylation in living cells will find wide applications in DNA methylation-related researches of toxicology, nutritional response, pathogen–host interaction, and antibacterial defense.

3. Conclusions and perspectives

DNA methylation is a critical post-transcriptional modification, and it plays crucial roles in epigenetic regulation of gene expression. Abnormal DNA methylation of genomic DNA is implicated in various

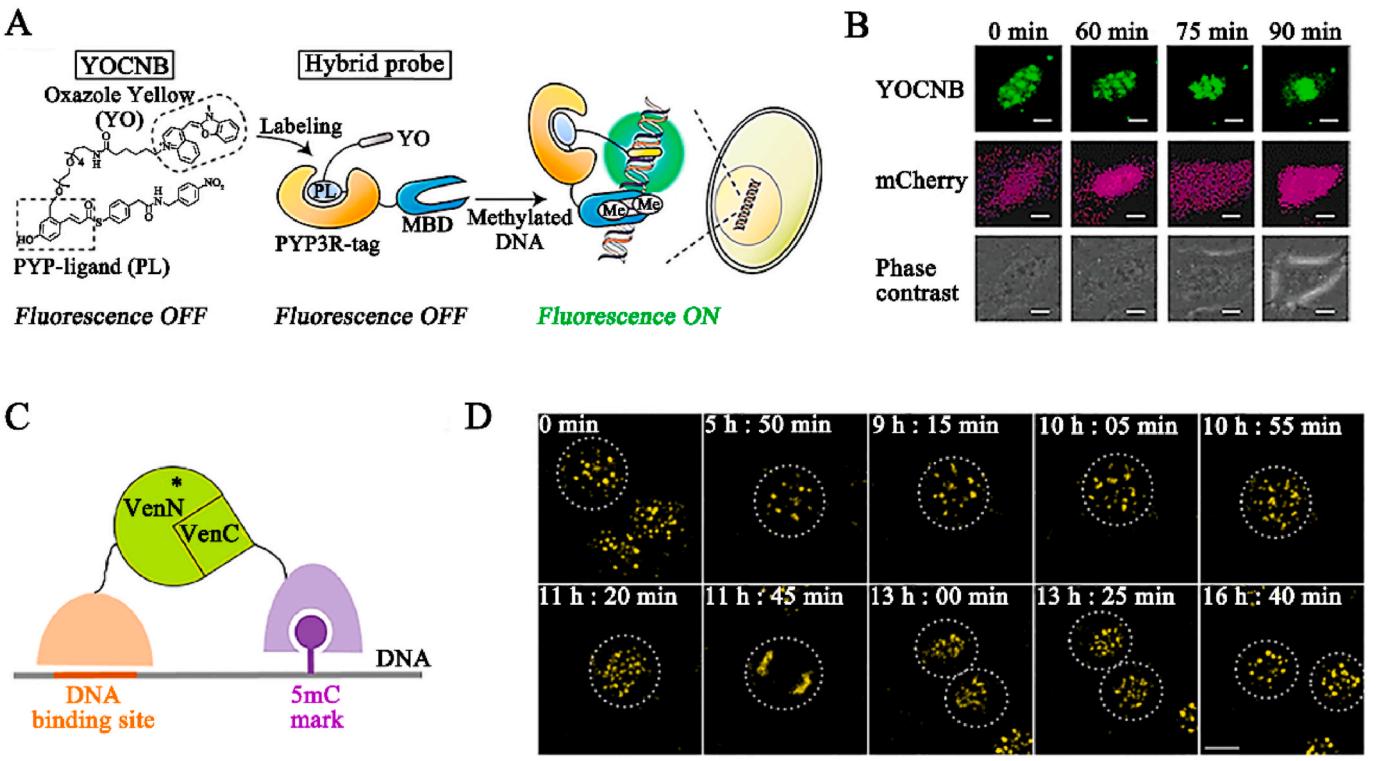

Fig. 7. (A) Principle of hybrid probe-based fluorescent biosensor for live-cell imaging of DNA methylation. (B) Real-time imaging of methylated DNA by using hybrid probe-based biosensor. Reproduced from Hori et al. (2018) with permission from American Chemical Society. (C) Principle of split fluorophore-based fluorescent biosensor for live-cell imaging of DNA methylation. (B) Real-time imaging of methylated DNA by using split fluorophore-based biosensor. Reproduced from Lungu et al. (2017) with permission from Nature Publishing Group.

human diseases including cancers. In the past five years (2015–2020), a series of novel biosensors have been developed for sensitive and selective detection of DNA methylation in vitro and even in living cells. In this review, we summarize the recent advances in biosensors for in vitro detection and in vivo imaging of 5-mC DNA methylation. The biosensors for in vitro detection of DNA methylation are categorized into fluorescent (Ma et al., 2015; Sun et al., 2018; Wang et al., 2018; Wu et al., 2016; Xu et al., 2016), electrochemical (Chen et al. 2017a, 2019; Feng et al. 2019, 2020; Huang et al., 2019; Wang et al., 2017b), colorimetric (Li et al., 2018; Su et al., 2015a), SERS (Wang et al., 2015, 2016b), MS (Lin et al., 2016), and SPR biosensors (Huertas et al., 2018), while the biosensors for in vivo imaging of DNA methylation is rarely available and they mainly rely on fluorescent imaging (Hori et al., 2018; Lungu et al., 2017). These biosensors facilitate the DNA methylation-related biological and biomedical researches, disease diagnosis, and drug discovery. Moreover, we assess the suitability of these biosensors for point-of-care testing (POCT) by comprehensive evaluation of the assay complexity, cost, analysis time, performance (including detection range, sensitivity, and repeatability), and real sample analysis capability (Table 1). Among them, the fluorescent biosensor based on DNA strand exchange (Xu et al., 2016), electrochemical biosensor based on MB (Povedano et al., 2019), electrochemical biosensor based on MB and multiple HRPs-modified antibody (Povedano et al., 2020), and SPR biosensor based on PPRH probe (Huertas et al., 2018) are most promising for POCT applications due to their distinct features including the avoidance of bisulfite treatment, the elimination of any enzymes, simple operation, low cost, low sample consumption, and good assay performance.

However, there are still some limitations that remain to be solved in the development of biosensors for DNA methylation assay. (1) The bisulfite conversion is the gold standard method for DNA methylation assay, but the requirement of harsh chemical treatment and relatively laborious and time-consuming procedures greatly limit their wide applications. (2) Restriction endonucleases have been successfully used for DNA methylation recognition, however only few DNA methylation-specific endonucleases (e.g., HpaII, GlaI, and BbvI.) are currently available (Table 1). (3) To improve the detection sensitivity, nucleic acid amplification strategies including PCR, LCR, and EXPAR are employed for the amplification of DNA methylation signal, but they are usually expensive with the involvement of complicated procedures due to the requirement of specific enzymes (e.g., polymerase, ligase, and nicking enzymes) to achieve the signal amplification. (4) The biosensors for in vivo imaging of DNA methylation are rarely reported and they mainly exploit recombinant proteins as the fluorescent labels and recognition elements (Hori et al., 2018; Lungu et al., 2017). Nevertheless, the construction of recombinant protein is technically difficult and relatively cumbersome. (5) Most biosensors are suitable for 5-mC detection, but few biosensors are available for the detection of other methylation types such as 5-hmC, 5-fC, and 5-caC.

To solve these issues, great efforts should be made in the future research. (1) Some bisulfite-free conversion methods are established based on Friedländer synthesis reaction (Xia et al., 2015) and the combination of ten-eleven translocation (TET) oxidation and pyridine borane reduction (Liu et al., 2019b). The development of new bisulfite-free conversion methods and further adoption of them in biosensors development will greatly facilitate DNA methylation profiling. (2) The discovery of new methylation-sensitive restriction endonuclease is required to facilitate the detection of DNA methylation existed in different sequences and locations. (3) With the development of DNA nanotechnology, DNA machines (e.g., hybridization chain reaction (Chen et al., 2019), entropy-driven reaction (Liang et al., 2017) and catalytic hairpin assembly (Karunanayake Mudiyanselage et al., 2018)) enable efficient signal amplification without the usage of any enzymes, with potential application in the amplified biosensing of DNA methylation. (4) Nanomaterials are attractive in bioimaging applications due to their excellent size-dependent optical, chemical, electronic, and mechanical features, and a series of nanomaterials such as QDs (Muro et al.,

Table 1
Summary of biosensors for in vitro detection of DNA methylation [a].

Strategy	Target discrimination approach	Detection range	Detection limit	Real sample type	Suitability for POCT	Ref.
Fluorescent biosensor based on QD	HpaII digestion	ND	ND	lung cancer tissue	medium	Ma et al. (2015)
Fluorescent biosensor based on UCNP and AuNR	HpaII digestion	0–100 nM	7 pM	ND	low	Wu et al. (2016)
Fluorescent biosensor based on EXPAR	GlaI digestion	200 aM - 200 pM	200 aM	ND	low	Sun et al. (2018)
Fluorescent biosensor based on DNA strand exchange	strand exchange kinetic	ND	ND	ND	high	Xu et al. (2016)
Fluorescent biosensor based on single-molecule detection	bisulfite treatment	10 aM - 10 pM	1 aM	lung cancer cells H157 and H209	medium	Wang et al. (2018)
Electrochemical biosensor based on paired-end tagging	bisulfite treatment	50 pg - 5 ng	40 pg	lung cancer plasma	medium	Chen et al. (2017a)
Electrochemical biosensor based on Exo III digestion	bisulfite treatment	10 fM - 100 pM	4 fM	ND	low	Feng et al. (2020)
Electrochemical biosensor based on tetrahedral DNA	bisulfite treatment	3–150 pg	ND	lung cancer plasma	medium	Wang et al. (2017b)
Electrochemical biosensor based on supersandwich DNA structure	bisulfite treatment	10 fM - 1 nM	450 aM	ND	medium	Feng et al. (2019)
Electrochemical biosensor based on tetrahedral DNA and HCR	HpaII digestion	1 aM - 100 nM	0.93 aM	ND	medium	Chen et al. (2019)
Electrochemical biosensor based on GO	antibody recognition	1 fM - 10 nM	1 fM	ND	medium	Huang et al. (2019)
Electrochemical biosensor based on MB	antibody recognition	4.0 pM–250 pM for 5-mC, 1.44 pM–100 pM for 5-hmC	1.2 pM for 5-mC, 0.43 pM for 5-hmC	U-87, SW48, and SW620 cells, colorectal cancer tissue	high	Povedano et al. (2019)
Electrochemical biosensor based on MB and multiple HRPs-modified antibody	antibody recognition	77 pM–7500 pM using ProtA−polyHRP80, 44 pM–5000 pM using Histostar	23 pM using ProtA−polyHRP$_{80}$, 13 pM using Histostar	colorectal cancer cell, tissue	high	Povedano et al. (2020)
Colorimetric biosensor based on AuNP	bisulfite treatment	0.01–1 fM	0.01 fM	healthy volunteer blood	low	Su et al. (2015a)
Colorimetric biosensor based on DNAzyme	bisulfite treatment	100 - 107 copies	100 copies	hepatoma cell HepG2	medium	Li et al. (2018)
SERS biosensor based on LCR	bisulfite treatment	0.5–500 pM	0.5 pM	breast cancer cells MDA-MB 231, MDA-MB 468, and HCC 1937	medium	Wang et al. (2015)
SERS biosensor based on MBD	HpaII digestion	20–1000 pg	200 pg	breast cancer tissue	medium	Wang et al. (2016b)
MS biosensor based on target fragmentation assay	BbvI. digestion	0.5–200 pM	0.11 pM	prostate tissue	medium	Lin et al. (2016)
SPR biosensor based on PPRH probe	antibody recognition	0–50 nM	115 pM	ND	high	Huertas et al. (2018)

2010), AuNPs (Sun et al., 2010), graphene oxide (Sun et al., 2008), and silver nanocluster (Yu et al., 2007) have been successfully applied of the imaging of intracellular biomolecules. The introduction of functional nanomaterials may greatly simplify the protocols and improve the performance of DNA methylation imaging. (5) Recent studies show that 5-mC can be oxidized by ten-eleven translocation (TET) enzymes to successively produce 5hmC, 5 fC and 5caC, and subsequently 5 fC and 5caC can be excised by thymidine DNA glycosidase to restore unmodified C, leading to the demethylation of methylated DNA (Maiti and Drohat, 2011). Although it is hypothesized that 5hmC, 5 fC and 5caC can serve as the stable epigenetic markers (Chen et al., 2017b), their biological roles are largely unknown because their abundance is extremely low and difficult to be accurately detected. The available methods for 5hmC, 5 fC and 5caC detection mainly rely on mass spectrometry (Zhang et al., 2016), thin layer chromatography (Khare et al., 2012), immunoprecipitation (Jin et al., 2011), and DNA sequencing (Neri et al., 2016), which may suffer from the sophisticated instruments, complicated labeling, laborious procedures, and long assay time. Therefore, the development of novel biosensors for sensitive and accurate detection of 5hmC, 5 fC and 5caC is urgently required for deeper understanding their biological roles and clinical relevance. With the devotion of these efforts, we believe that the DNA methylation biosensors will greatly contribute to fundamental biomedical researches, clinical applications and drug discovery in the near future.

Declaration of competing interest

The authors declare that they have no known competing financial interests or personal relationships that could have appeared to influence the work reported in this paper.

Acknowledgments

This work was supported by the National Natural Science Foundation of China (Grant No. 21527811, 21735003 and 21705096) and the Award for Team Leader Program of Taishan Scholars of Shandong Province, China.

References

Alley Jr., W.R., Mann, B.F., Novotny, M.V., 2013. Chem. Rev. 113 (4), 2668–2732.
Andrew, P., Barnes, W.L., 2000. Science 290 (5492), 785–788.
Angel, T.E., Aryal, U.K., Hengel, S.M., Baker, E.S., Kelly, R.T., Robinson, E.W., Smith, R. D., 2012. Chem. Soc. Rev. 41 (10), 3912–3928.
Aoki, H., Corn, R.M., Matthews, B., 2019. Biosens. Bioelectron. 142, 111565.
Avci-Adali, M., Paul, A., Wilhelm, N., Ziemer, G., Wendel, H.P., 2009. Molecules 15 (1), 1–11.
Barany, F., 1991. Proc. Natl. Acad. Sci. Unit. States Am. 88 (1), 189–193.
Bird, A., 2002. Genes Dev. 16 (1), 6–21.
Boltze, C., Zack, S., Quednow, C., Bettge, S., Roessner, A., Schneider-Stock, R., 2003. Pathol. Res. Pract. 199 (6), 399–404.
Campuzano, S., Pedrero, M., Yánez-Sedeño, P., Pingarrón, J.M., 2019. Electroanalysis 31 (10), 1816–1832.
Capper, D., Jones, D.T.W., Sill, M., Hovestadt, V., Schrimpf, D., Sturm, D., Koelsche, C., Sahm, F., Chavez, L., Reuss, D.E., Kratz, A., Wefers, A.K., Huang, K., Pajtler, K.W., Schweizer, L., Stichel, D., Olar, A., Engel, N.W., Lindenberg, K., Harter, P.N., Braczynski, A.K., Plate, K.H., Dohmen, H., Garvalov, B.K., Coras, R., Hölsken, A., Hewer, E., Bewerunge-Hudler, M., Schick, M., Fischer, R., Beschorner, R., Schittenhelm, J., Staszewski, O., Wani, K., Varlet, P., Pages, M., Temming, P., Lohmann, D., Selt, F., Witt, H., Milde, T., Witt, O., Aronica, E., Giangaspero, F., Rushing, E., Scheurlen, W., Geisenberger, C., Rodriguez, F.J., Becker, A., Preusser, M., Haberler, C., Bjerkvig, R., Cryan, J., Farrell, M., Deckert, M., Hench, J., Frank, S., Serrano, J., Kannan, K., Tsirigos, A., Brück, W., Hofer, S., Brehmer, S., Seiz-Rosenhagen, M., Hänggi, D., Hans, V., Rozsnoki, S., Hansford, J.R., Kohlhof, P., Kristensen, B.W., Lechner, M., Lopes, B., Mawrin, C., Ketter, R., Kulozik, A., Khatib, Z., Heppner, F., Koch, A., Jouvet, A., Keohane, C., Mühleisen, H., Mueller, W., Pohl, U., Prinz, M., Benner, A., Zapatka, M., Gottardo, N.G., Driever, P. H., Kramm, C.M., Müller, H.L., Rutkowski, S., von Hoff, K., Frühwald, M.C., Gnekow, A., Fleischhack, G., Tippelt, S., Calaminus, G., Monoranu, C.-M., Perry, A., Jones, C., Jacques, T.S., Radlwimmer, B., Gessi, M., Pietsch, T., Schramm, J., Schackert, G., Westphal, M., Reifenberger, G., Wesseling, P., Weller, M., Collins, V. P., Blümcke, I., Bendszus, M., Debus, J., Huang, A., Jabado, N., Northcott, P.A., Paulus, W., Gajjar, A., Robinson, G.W., Taylor, M.D., Jaunmuktane, Z., Ryzhova, M., Platten, M., Unterberg, A., Wick, W., Karajannis, M.A., Mittelbronn, M., Acker, T., Hartmann, C., Aldape, K., Schüller, U., Buslei, R., Lichter, P., Kool, M., Herold-Mende, C., Ellison, D.W., Hasselblatt, M., Snuderl, M., Brandner, S., Korshunov, A., von Deimling, A., Pfister, S.M., 2018. Nature 555 (7697), 469–474.
Cavalli, G., Heard, E., 2019. Nature 571 (7766), 489–499.
Chen, F., Wang, X.Y., Cao, X.W., Zhao, Y.X., 2017a. Anal. Chem. 89 (19), 10468–10473.
Chen, K., Zhang, J., Guo, Z., Ma, Q., Xu, Z., Zhou, Y., Xu, Z., Li, Z., Liu, Y., Ye, X., Li, X., Yuan, B., Ke, Y., He, C., Zhou, L., Liu, J., Ci, W., 2016. Cell Res. 26 (1), 103–118.
Chen, X., Huang, J., Zhang, S., Mo, F., Su, S.S., Li, Y., Fang, L.C., Deng, J., Huang, H., Luo, Z.X., Zheng, J.S., 2019. ACS Appl. Mater. Interfaces 11 (4), 3745–3752.
Chen, Y., Hong, T., Wang, S., Mo, J., Tian, T., Zhou, X., 2017b. Chem. Soc. Rev. 46 (10), 2844–2872.
Cheng, X., Roberts, R.J., 2001. Nucleic Acids Res. 29 (18), 3784–3795.
Chouliaras, L., Mastroeni, D., Delvaux, E., Grover, A., Kenis, G., Hof, P.R., Steinbusch, H. W., Coleman, P.D., Rutten, B.P., van den Hove, D.L., 2013. Neurobiol. Aging 34 (9), 2091–2099.
Dahl, C., Guldberg, P., 2003. Biogerontology 4 (4), 233–250.
Das, P.M., Singal, R., 2004. J. Clin. Oncol. 22 (22), 4632–4642.
Deng, G., Chen, A., Hong, J., Chae, H.S., Kim, Y.S., 1999. Canc. Res. 59 (9), 2029, 2023.
Ding, C., Tian, Y., 2015. Biosens. Bioelectron. 65, 183–190.
Dominguez-Salas, P., Moore, S.E., Baker, M.S., Bergen, A.W., Cox, S.E., Dyer, R.A., Fulford, A.J., Guan, Y., Laritsky, E., Silver, M.J., Swan, G.E., Zeisel, S.H., Innis, S.M., Waterland, R.A., Prentice, A.M., Hennig, B.J., 2014. Nat. Commun. 5, 3746.
Elghanian, R., Storhoff, J.J., Mucic, R.C., Letsinger, R.L., Mirkin, C.A., 1997. Science 277 (5329), 1078–1081.
Esteller, M., Corn, P.G., Baylin, S.B., Herman, J.G., 2001. Canc. Res. 61 (8), 3225–3229.
Fatemi, M., Wade, P.A., 2006. J. Cell Sci. 119 (Pt 15), 3033–3037.
Feng, Q., Qin, L., Wang, M., Wang, P., 2020. Biosens. Bioelectron. 149, 111847.
Feng, Q.M., Wang, M.Y., Qin, L., Wang, P., 2019. ACS Sens. 4 (10), 2615–2622.
Field, A.E., Robertson, N.A., Wang, T., Havas, A., Ideker, T., Adams, P.D., 2018. Mol. Cell 71 (6), 882–895.
Fraga, M.F., Esteller, M., 2002. Biotechniques 33 (3), 632–649.
Frommer, M., McDonald, L.E., Millar, D.S., Collis, C.M., Watt, F., Grigg, G.W., Molloy, P. L., Paul, C.L., 1992. Proc. Natl. Acad. Sci. U. S. A. 89 (5), 1827–1831.
Fu, L., Amato, N.J., Wang, P., McGowan, S.J., Niedernhofer, L.J., Wang, Y., 2015. Anal. Chem. 87 (15), 7653–7659.
Furstenberg, A., Deligeorgiev, T.G., Gadjev, N.I., Vasilev, A.A., Vauthey, E., 2007. Chem. Eur J. 13 (30), 8600–8609.
Ge, Z., Lin, M., Wang, P., Pei, H., Yan, J., Shi, J., Huang, Q., He, D., Fan, C., Zuo, X., 2014. Anal. Chem. 86 (4), 2124–2130.
Goedecke, S., Schlosser, S., Mühlisch, J., Hempel, G., Frühwald, M.C., Wünsch, B., 2009. Electrophoresis 30 (17), 3063–3070.
Gonzalgo, M.L., Jones, P.A., 1997. Nucleic Acids Res. 25 (12), 2529–2531.
Greally, J.M., 2018. Nat. Rev. Mol. Cell Biol. 19 (4), 207–208.
Herman, J.G., Graff, J.R., Myöhänen, S., Nelkin, B.D., Baylin, S.B., 1996. Proc. Natl. Acad. Sci. U. S. A. 93 (18), 9821–9826.
Holliday, R., 1987. Science 238 (4824), 163–170.
Hori, Y., Otomura, N., Nishida, A., Nishiura, M., Umeno, M., Suetake, I., Kikuchi, K., 2018. J. Am. Chem. Soc. 140 (5), 1686–1690.
Hsin, T.M., Yeung, E.S., 2007. Angew. Chem. Int. Ed. 46 (42), 8032–8035.
Hu, J., Zhang, C.-y., 2014. Chem. Commun. 50 (88), 13581–13584.
Huang, J., Zhang, S., Mo, F., Su, S., Chen, X., Li, Y., Fang, L., Huang, H., Deng, J., Liu, H., Yang, X., Zheng, J., 2019. Biosens. Bioelectron. 127, 155–160.
Huertas, C.S., Aviñó, A., Kurachi, C., Piqué, A., Sandoval, J., Eritja, R., Esteller, M., Lechuga, L.M., 2018. Biosens. Bioelectron. 120, 47–54.
Issa, J.-P., 2004. Nat. Rev. Canc. 4 (12), 988.
Jiang, Y., Liu, N., Guo, W., Xia, F., Jiang, L., 2012. J. Am. Chem. Soc. 134 (37), 15395–15401.
Jin, S.-G., Wu, X., Li, A.X., Pfeifer, G.P., 2011. Nucleic Acids Res. 39 (12), 5015–5024.
Karpinski, P., Szmida, E., Misiak, B., Ramsey, D., Leszczynski, P., Bebenek, M., Sedziak, T., Grzebieniak, Z., Jonkisz, A., Lebioda, A., 2012. Mol. Carcinog. 51 (12), 1003–1008.
Karunanayake Mudiyanselage, A.P.K.K., Yu, Q., Leon-Duque, M.A., Zhao, B., Wu, R., You, M., 2018. J. Am. Chem. Soc. 140 (28), 8739–8745.
Kato, D., Sekioka, N., Ueda, A., Kurita, R., Hirono, S., Suzuki, K., Niwa, O., 2008. J. Am. Chem. Soc. 130 (12), 3716–3717.
Khare, T., Pai, S., Koncevicius, K., Pal, M., Kriukiene, E., Liutkeviciute, Z., Irimia, M., Jia, P., Ptak, C., Xia, M., Tice, R., Tochigi, M., Moréra, S., Nazarians, A., Belsham, D., Wong, A.H.C., Blencowe, B.J., Wang, S.C., Kapranov, P., Kustra, R., Labrie, V., Klimasauskas, S., Petronis, A., 2012. Nat. Struct. Mol. Biol. 19 (10), 1037–1043.
Kitsera, N., Allgayer, J., Parsa, E., Geier, N., Rossa, M., Carell, T., Khobta, A., 2017. Nucleic Acids Res. 45 (19), 11033–11042.
Kneipp, K., Kneipp, H., Itzkan, I., Dasari, R.R., Feld, M.S., 1999. Chem. Rev. 99 (10), 2957–2976.
Kneipp, K., Wang, Y., Kneipp, H., Perelman, L.T., Itzkan, I., Dasari, R.R., Feld, M.S., 1997. Phys. Rev. Lett. 78 (9), 1667.
Koch, A., Joosten, S.C., Feng, Z., de Ruijter, T.C., Draht, M.X., Melotte, V., Smits, K.M., Veeck, J., Herman, J.G., Van Neste, L., Van Criekinge, W., De Meyer, T., van Engeland, M., 2018. Nat. Rev. Clin. Oncol. 15 (7), 459–466.
Kouzarides, T., 2007. Cell 128 (4), 693–705.
Krejcova, L., Richtera, L., Hynek, D., Labuda, J., Adam, V., 2017. Biosens. Bioelectron. 97, 384–399.
Kudr, J., Zhao, L., Nguyen, E.P., Arola, H., Nevanen, T.K., Adam, V., Zitka, O., Merkoçi, A., 2020. Biosens. Bioelectron. 156, 112109.
Kumar, M., Bijo, A.J., Baghel, R.S., Reddy, C.R., Jha, B., 2012. Plant Physiol. Biochem. 51, 129–138.
Laird, P.W., 2003. Nat. Rev. Canc. 3 (4), 253.
Li, D., Liu, J., Barrow, C.J., Yang, W., 2014. Chem. Commun. 50 (60), 8197–8200.
Li, M., Zhang, L., Chen, G.Y., Zhou, J., Yuan, Y., Zou, J.W., Yuan, M.M., Chen, R., Du, F., Cui, X., Huang, X., Dong, J., Tang, Z., 2018. Chem. Commun. 54 (14), 1710–1713.
Li, Q., Ahuja, N., Burger, P.C., Issa, J.-P.J., 1999. Oncogene 18 (21), 3284.
Li, T., Dong, S., Wang, E., 2010a. J. Am. Chem. Soc. 132 (38), 13156–13157.
Li, T., Wang, E., Dong, S., 2010b. Anal. Chem. 82 (4), 1515–1520.
Liang, C.-P., Ma, P.-Q., Liu, H., Guo, X., Yin, B.-C., Ye, B.-C., 2017. Angew. Chem. Int. Ed. 56 (31), 9077–9081.
Liang, G., Gonzalgo, M.L., Salem, C., Jones, P.A., 2002. Methods 27 (2), 150–155.
Liang, L., Li, J., Li, Q., Huang, Q., Shi, J., Yan, H., Fan, C., 2014. Angew. Chem. Int. Ed. 53 (30), 7745–7750.
Lin, X.C., Zhang, T., Liu, L., Tang, H., Yu, R.Q., Jiang, J.H., 2016. Anal. Chem. 88 (2), 1083–1087.
Liu, H., Luo, J., Fang, L., Huang, H., Deng, J., Huang, J., Zhang, S., Li, Y., Zheng, J., 2018a. Biosens. Bioelectron. 121, 47–53.
Liu, M., Ma, F., Zhang, Q., Zhang, C.-y., 2018b. Chem. Commun. 54 (13), 1583–1586.
Liu, N., Jiang, Y., Zhou, Y., Xia, F., Guo, W., Jiang, L., 2013. Angew. Chem. Int. Ed. 52 (7), 2007–2011.
Liu, W.-J., Xu, Q., Ma, F., Li, C.-C., Zhang, C.-Y., 2018c. Analyst 143 (22), 5461–5466.
Liu, Y., Ge, Z., Chen, M., He, H., Zhang, X., Wang, S., 2019a. Biosens. Bioelectron. 142, 111537.
Liu, Y., Siejka-Zielińska, P., Velikova, G., Bi, Y., Yuan, F., Tomkova, M., Bai, C., Chen, L., Schuster-Böckler, B., Song, C.-X., 2019b. Nat. Biotechnol. 37 (4), 424–429.
Liu, Z., Lei, S., Zou, L., Li, G., Ye, B., 2020. Biosens. Bioelectron. 167, 112487.
Lungu, C., Pinter, S., Broche, J., Rathert, P., Jeltsch, A., 2017. Nat. Commun. 8 (1), 649.
Ma, F., Li, C.-c., Zhang, C.-y., 2018. J. Mater. Chem. B 6 (39), 6173–6190.
Ma, F., Li, Y., Tang, B., Zhang, C.-y., 2016a. Acc. Chem. Res. 49 (9), 1722–1730.
Ma, F., Liu, M., Wang, Z.-y., Zhang, C.-y., 2016b. Chem. Commun. 52 (6), 1218–1221.
Ma, F., Liu, M., Zhang, C.-y., 2019. Chem. Commun. 55 (61), 8963–8966.
Ma, F., Yang, Y., Zhang, C.-y., 2014. Anal. Chem. 86 (12), 6006–6011.
Ma, Y.F., Zhang, H.L., Liu, F.M., Wu, Z.H., Lu, S.H., Jin, Q.H., Zhao, J.L., Zhong, X.H., Mao, H.J., 2015. Nanoscale 7 (41), 17547–17555.
Maiti, A., Drohat, A.C., 2011. J. Biol. Chem. 286 (41), 35334–35338.
Martinez, G., Castellano, M., Tortosa, M., Pallas, V., Gomez, G., 2013. Nucleic Acids Res. 42 (3), 1553–1562.
Masters, B.R., 2008. J. Biomed. Optic. 13 (2), 029901.
Medintz, I.L., Uyeda, H.T., Goldman, E.R., Mattoussi, H., 2005. Nat. Mater. 4 (6), 435.
Miyamoto, K., Fukutomi, T., Akashi-Tanaka, S., Hasegawa, T., Asahara, T., Sugimura, T., Ushijima, T., 2005. Int. J. Canc. 116 (3), 407–414.
Muro, E., Pons, T., Lequeux, N., Fragola, A., Sanson, N., Lenkei, Z., Dubertret, B., 2010. J. Am. Chem. Soc. 132 (13), 4556–4557.
Nassiri, F., Chakravarthy, A., Feng, S., Shen, S.Y., Nejad, R., Zuccato, J.A., Voisin, M.R., Patil, V., Horbinski, C., Aldape, K., Zadeh, G., De Carvalho, D.D., 2020. Nat. Med. 26 (7), 1044–1047.
Nazmul Islam, M., Yadav, S., Hakimul Haque, M., Munaz, A., Islam, F., Al Hossain, M.S., Gopalan, V., Lam, A.K., Nguyen, N.-T., Shiddiky, M.J.A., 2017. Biosens. Bioelectron. 92, 668–678.
Neri, F., Incarnato, D., Krepelova, A., Parlato, C., Oliviero, S., 2016. 11(7), 1191-1205.
Neri, F., Rapelli, S., Krepelova, A., Incarnato, D., Parlato, C., Basile, G., Maldotti, M., Anselmi, F., Oliviero, S., 2017. Nature 543 (7643), 72–77.

Pal, S., Tyler, J.K., 2016. Sci. Adv. 2 (7), e1600584.
Povedano, E., Montiel, V.R.-V., Valverde, A., Navarro-Villoslada, F., Yáñez-Sedeño, P., Pedrero, M., Montero-Calle, A., Barderas, R., Peláez-García, A., Mendiola, M., Hardisson, D., Feliú, J., Camps, J., Rodríguez-Tomàs, E., Joven, J., Arenas, M., Campuzano, S., Pingarrón, J.M., 2019. ACS Sens. 4 (1), 227–234.
Povedano, E., Ruiz-Valdepeñas Montiel, V., Gamella, M., Pedrero, M., Barderas, R., Peláez-García, A., Mendiola, M., Hardisson, D., Feliú, J., Yáñez-Sedeño, P., Campuzano, S., Pingarrón, J.M., 2020. Anal. Chem. 92 (7), 5604–5612.
Ramsahoye, B.H., Burnett, A.K., Taylor, C., 1997. Nucleic Acids Res. 25 (16), 3196–3198.
Reik, W., Dean, W., Walter, J., 2001. Science 293 (5532), 1089–1093.
Resch-Genger, U., Grabolle, M., Cavaliere-Jaricot, S., Nitschke, R., Nann, T., 2008. Nat. Methods 5 (9), 763.
Rich, R.L., Myszka, D.G., 2000. Curr. Opin. Biotechnol. 11 (1), 54–61.
Rohde, C., Zhang, Y., Jurkowski, T.P., Stamerjohanns, H., Reinhardt, R., Jeltsch, A., 2008. Nucleic Acids Res. 36 (5), e34.
Rosi, N.L., Mirkin, C.A., 2005. Chem. Rev. 105 (4), 1547–1562.
Schlücker, S., 2009. ChemPhysChem 10 (9-10), 1344–1354.
Shinagawa, S., Kobayashi, N., Nagata, T., Kusaka, A., Yamada, H., Kondo, K., Nakayama, K., 2016. Neurosci. Lett. 629, 33–37.
Singer-Sam, J., LeBon, J.M., Tanguay, R.L., Riggs, A.D., 1990. Nucleic Acids Res. 18 (3), 687.
Smith, A.E., Ford, K.G., 2006. Nucleic Acids Res. 35 (3), 740–754.
Somers, R.C., Bawendi, M.G., Nocera, D.G., 2007. Chem. Soc. Rev. 36 (4), 579–591.
Song, C.-X., Diao, J., Brunger, A.T., Quake, S.R., 2016. Proc. Natl. Acad. Sci. U. S. A. 113 (16), 4338–4343.
Storhoff, J.J., Elghanian, R., Mucic, R.C., Mirkin, C.A., Letsinger, R.L., 1998. J. Am. Chem. Soc. 120 (9), 1959–1964.
Stryer, L., 1978. Annu. Rev. Biochem. 47 (1), 819–846.
Su, F.X., Wang, L.M., Sun, Y.Y., Liu, C.H., Duan, X.R., Li, Z.P., 2015a. Chem. Commun. 51 (16), 3371–3374.
Su, X., Chu, Y., Kordower, J.H., Li, B., Cao, H., Huang, L., Nishida, M., Song, L., Wang, D., Federoff, H.J., 2015b. PloS One 10 (8), e0134087.
Sun, I.-C., Lee, S., Koo, H., Kwon, I.C., Choi, K., Ahn, C.-H., Kim, K., 2010. Bioconjugate Chem. 21 (11), 1939–1942.
Sun, X., Liu, Z., Welsher, K., Robinson, J.T., Goodwin, A., Zaric, S., Dai, H., 2008. Nano Res 1 (3), 203–212.
Sun, Y.Y., Sun, Y.Y., Tian, W.M., Liu, C.H., Gao, K.J., Li, Z.P., 2018. Chem. Sci. 9 (5), 1344–1351.
Susan, J.C., Harrison, J., Paul, C.L., Frommer, M., 1994. Nucleic Acids Res. 22 (15), 2990–2997.
Syedmoradi, L., Esmaeili, F., Norton, M.L., 2016. Analyst 141 (21), 5922–5943.
Taleat, Z., Mathwig, K., Sudhölter, E.J.R., Rassaei, L., 2015. TrAC Trends Anal. Chem. (Reference Ed.) 66, 80–89.
Tanaka, K., Okamoto, A., 2007. Bioorg. Med. Chem. Lett 17 (7), 1912–1915.
Tarasova, G.V., Nayakshina, T.N., Degtyarev, S.K., 2008. BMC Mol. Biol. 9, 7.
Taylor, S.E., Smeriglio, P., Dhulipala, L., Rath, M., Bhutani, N., 2014. Arthritis Rheum. 66 (1), 90–100.
Tucker, D.W., Getchell, C.R., McCarthy, E.T., Ohman, A.W., Sasamoto, N., Xu, S., Ko, J. Y., Gupta, M., Shafrir, A., Medina, J.E., Lee, J.J., MacDonald, L.A., Malik, A., Hasselblatt, K.T., Li, W., Zhang, H., Kaplan, S.J., Murphy, G.F., Hirsch, M.S., Liu, J. F., Matulonis, U.A., Terry, K.L., Lian, C.G., Dinulescu, D.M., 2018. Clin. Canc. Res. 24 (6), 1389–1401.
Vanaja, D.K., Ehrich, M., Van den Boom, D., Cheville, J.C., Karnes, R.J., Tindall, D.J., Cantor, C.R., Young, C.Y., 2009. Canc. Invest. 27 (5), 549–560.
Walt, D.R., 2012. Anal. Chem. 85, 1258–1263.
Wang, J., Yuan, B., Guerrero, C., Bahde, R., Gupta, S., Wang, Y., 2011. Anal. Chem. 83 (6), 2201–2209.
Wang, L.-j., Zhang, Q., Tang, B., Zhang, C.-y., 2017a. Anal. Chem. 89 (13), 7255–7261.
Wang, L.Y., Yan, R.X., Hao, Z.Y., Wang, L., Zeng, J.H., Bao, J., Wang, X., Peng, Q., Li, Y. D., 2005. Angew. Chem. Int. Ed. 44 (37), 6054–6057.
Wang, S., Song, J., Yang, Y., Zhang, Y., Wang, H., Ma, J., 2016a. PloS One 10 (12), e0145944.
Wang, X.Y., Chen, F., Zhang, D.X., Zhao, Y., Wei, J., Wang, L.H., Song, S.P., Fan, C.H., Zhao, Y.X., 2017b. Chem. Sci. 8 (7), 4764–4770.
Wang, Y., Schlücker, S., 2013. Analyst 138 (8), 2224–2238.
Wang, Y.L., Wee, E.J.H., Trau, M., 2015. Chem. Commun. 51 (54), 10953–10956.
Wang, Y.L., Wee, E.J.H., Trau, M., 2016b. Chem. Commun. 52 (17), 3560–3563.
Wang, Z.Y., Wang, L.J., Zhang, Q.Y., Tang, B., Zhang, C.Y., 2018. Chem. Sci. 9 (5), 1330–1338.
Wei, Z., Han, S., Gong, X., Zhao, Y., Yang, C., Zhang, S., Zhang, X., 2013. Angew. Chem. Int. Ed. 52 (42), 11025–11028.
Wu, M.M., Wang, X.Y., Wang, K., Guo, Z.J., 2016. Chem. Commun. 52 (54), 8377–8380.
Wu, S.W., Han, G., Milliron, D.J., Aloni, S., Altoe, V., Talapin, D.V., Cohen, B.E., Schuck, P.J., 2009. Proc. Natl. Acad. Sci. U. S. A 106 (27), 10917–10921.
Xia, B., Han, D., Lu, X., Sun, Z., Zhou, A., Yin, Q., Zeng, H., Liu, M., Jiang, X., Xie, W., He, C., Yi, C., 2015. Nat. Methods 12 (11), 1047–1050.
Xiong, Z., Laird, P.W., 1997. Nucleic Acids Res. 25 (12), 2532–2534.
Xu, C., Wu, J.J., Liu, W.T., Hong, T.T., Wang, T.L., Zhang, X.E., Fu, B.S., Wu, F., Wu, Z.G., Zhou, X., 2016. Chem. Commun. 52 (41), 6833–6836.
Xu, X.-H., Yeung, E.S., 1997. Science 275 (5303), 1106–1109.
Yu, A., Lepère, G., Jay, F., Wang, J., Bapaume, L., Wang, Y., Abraham, A.-L., Penterman, J., Fischer, R.L., Voinnet, O., Navarro, L., 2013. Proc. Natl. Acad. Sci. U. S. A. 110 (6), 2389–2394.
Yu, J., Patel, S.A., Dickson, R.M., 2007. Angew. Chem. Int. Ed. 46 (12), 2028–2030.
Zhang, L., Li, Z., Chen, G., Huang, Q., Zhang, J., Wen, J., Ye, X., Cai, C., 2016. Anal. Methods 8 (29), 5812–5817.
Zhang, L., Xu, Y.-Z., Xiao, X.-F., Chen, J., Zhou, X.-Q., Zhu, W.-Y., Dai, Z., Zou, X.-Y., 2015. TrAC Trends Anal. Chem. (Reference Ed.) 72, 114–122.
Zhang, Y., Chen, Y., Qu, H., Wang, Y., 2019. Mol. Genet. Genom. Med. 7 (4), e00583.
Zhao, Y., Chen, F., Li, Q., Wang, L., Fan, C., 2015. Chem. Rev. 115 (22), 12491–12545.
Zhou, J., Qi, Q., Wang, C., Qian, Y., Liu, G., Wang, Y., Fu, L., 2019. Biosens. Bioelectron. 142, 111449.
Zhou, J., Wang, Q.-x., Zhang, C.-y., 2013. J. Am. Chem. Soc. 135 (6), 2056–2059.
Zhou, M., Zhai, Y., Dong, S., 2009. Anal. Chem. 81 (14), 5603–5613.